RESIDUAL STRESSES IN TAILOR WELDED BLANKS DUE TO SPRINGBACK AFTER BENDING

A DISSERTATION

SUBMITTED IN PARTIAL FULFILLMENT OF THE REQUIREMENTS FOR

THE AWARD OF THE DEGREE OF

MASTER OF TECHNOLOGY
IN
PRODUCTION ENGINEERING

SUBMITTED BY

HEMANT KUMAR
ROLL NO.-2K16/PIE/08

Under the supervision of

Dr. Vijay Gautam
PROFESSOR

Dr. (Mrs.) Reeta Wattal
PROFESSOR

DEPARTMENT OF MECHANICAL ENGINEERING
DELHI TECHNOLOGICAL UNIVERSITY
(Formerly Delhi College of Engineering)
Bawana Road, Delhi-110042
JULY, 2018

DELHI TECHNOLOGICAL UNIVERSITY

(Formerly Delhi College of Engineering)

Bawana Road, Delhi-110042

CANDIDATE'S DECLARATION

I, HEMANT KUMAR, Roll No. 2K16/PIE/08 student of M.Tech (Production Engineering), hereby declare that the project Dissertation titled "Residual stresses in Tailor Welded Blanks due to Springback after Bending" which is submitted by me to the Department of Mechanical Engineering, Delhi Technological University, Delhi in partial fulfillment of the requirement for the award of the degree of Master of Technology, is original and not copied from any source without proper citation. This work has not previously formed the basis for the award of any Degree, Diploma Associateship, Fellowship or other similar title or recognition.

Place: Delhi **HEMANT KUMAR**

Date: **Roll No. 2K16/PIE/08**

DELHI TECHNOLOGICAL UNIVERSITY

(Formerly Delhi College of Engineering)

Bawana Road, Delhi-110042

CERTIFICATE

I hereby certify that the project Dissertation titled "Residual stresses in Tailor Welded Blanks due to Springback after Bending" which is submitted by HEMANT KUMAR, Roll No. 2K16/PIE/08 Department of Mechanical Engineering, Delhi Technological University, Delhi in partial fulfillment of the requirement for the award of degree of Master of Technology, is a record of the project work carried out by the student under our supervision. To the best of our knowledge this work has not been submitted in part or full for any Degree or Diploma to this University or elsewhere.

Supervisor

Prof. VIJAY GAUTAM

Department Of Mechanical Engineering
Delhi Technological University
New Delhi-110042

Supervisor

Prof. REETA WATTAL

Department Of Mechanical Engineering
Delhi Technological University
New Delhi-110042

Place: Delhi

Date:

ACKNOWLEDGEMENT

Any accomplishment is a result of positivity of thoughts and efforts. It is important here to appreciate contribution, encouragement and support from persons who stood as 'Light House' throughout the voyage.

I wish to express my sincere gratitude for my project supervisor and mentor, Prof. Vijay Gautam and Prof. Reeta Wattal, Department of Mechanical Engineering, Delhi Technological University (Delhi). It was a golden opportunity to work under their kind supervision. Their scholastic guidance and sagacious suggestions helped me to complete the project.

I wish to thank Dr. Vipin, Head, Department of Mechanical Engineering, Delhi Technological University (Delhi), for constantly motivating and providing able guidance.

I am also thankful to the staff of Department of Mechanical Engineering for their continual support and cooperation.

Finally, but importantly, I would like to express my heartfelt thanks to my beloved family and friends who have endured the long working hours and whose motivation kept me going.

Place: Delhi

Date**:**

HEMANT KUMAR

Roll No. 2K16/PIE/08

M.Tech (Production Engineering)

Delhi Technological University, Delhi, India

ABSTRACT

Residual Stress is a stress that remains inside of a component after the original cause of stresses has been removed. These stresses are locked-in stresses in the material that is free of external forces and thermal gradients. These stresses self-equilibrate within the cross-section of the material and can result in unexpected failure if not accounted for. A Tailor Weld Blank is a flat sheet made by joining different pieces of metal either of dissimilar materials or different size, shape and thicknesses. The presence of weld zone and different thickness combination results in generation of residual stress in the blank which affect the forming behavior of tailor-welded blanks significantly. A good knowledge of variation, nature and magnitude of the residual stresses and of its distribution within the component is of great importance for the accurate assessment and evaluation of fatigue life of the cold formed components.

The present study is based on the experimental characterization and numerical analysis of residual stresses in the tailor welded blanks prepared by Nd-YAG laser welding of interstitial free steel with a thickness combination of 0.8mmX1.5mm, after springback a non-destructive cosα technique using a portable X-ray device (μ-X360 residual stress analyzer) is used to measure the residual stress in the tailor welded blanks experimentally. The longitudinally welded specimens of tailor welded blanks are tested on V-bending set-up with three different punch profile radii i.e. 10mm, 12.5mm and 15mm and the residual stress is measured on inner and outer side of the tested samples. The effect of the punch profile radius on residual stress before and after springback is observed to be very significant in bending of tailor welded blanks. As the punch profile radius increases, it is observed that residual stress decreases for a given thickness combination. The residual stress predicted by simulations agreed well with the experimental results for all punch radii.

Keywords: Residual stress, fatigue life, tailor welded blanks, cosα technique, X-ray device, punch profile radius.

TABLE OF CONTENTS

LIST OF FIGURES

LIST OF TABLES

LIST OF SYMBOLS

Symbol	Description
$d_{\phi\Psi}$	Inter-planar spacing of planes at an angle ψ to the surface.
d_o	Stress free inter-planar spacing.
ϕ(phi)	Angle between a fixed direction in the plane of the sample and the projection in that plane of the normal of the diffracting plane.
ψ (psi)	Angle between the normal of the sample and the normal of the diffracting plane (bisecting the incident and diffracted beams).
ψ_o	Angle of incident X-rays.
θ	Angle of the diffraction according to Bragg's Law.
$\varepsilon_{\phi\psi}$	Strain measured in the direction of measurement defined by the angles ϕ, ψ
E	Elastic modulus.
ν	Poisson's ratio.
λ	Wavelength of the X-ray.
α	Angle between incident X-ray and the diffracted ray impinged on the imaging plate to form debye ring.
ε_α	The strain projected along a direction with angle α.
n	Diffraction vector.

n_1, n_2, n_3	Directional cosines of the normal of the diffracting plane with respect to the axes in the sample coordinates
σ	Normal stress.
σ_ϕ	Stress acting in a chosen direction i.e. at an angle φ.

CHAPTER 1

INTRODUCTION

1.1 Introduction of Tailor Welded Blanks

A Tailor Weld Blank is a flat sheet made by joining different pieces of metal together either of dissimilar materials or different shape, size and thicknesses, to select and strengthen critical areas of the body without increasing significant weight of the component. Pieces of metals welded together by different welding processes like laser welding, plasma welding, arc welding etc. Laser welding is one of the best suited welding process for the production of tailor welded blanks as they are very narrow, have no raised top- or under-bead and do not require special machining .

Tailor Weld Blanks are semi-finished parts, which are made from sheets of similar or dissimilar materials having different shape, size, thicknesses, coatings or material properties. After joining, these will be subjected to different types of forming process such as bending, deep drawing, stamping etc. The concept of Tailored blanks were developed by ThyssenKrupp (a German steel manufacturing company) to make sheets that were wider than those made on available rolling mills of the time. Nowadays, TWBs are used in a very frequent manner to make different types of automotive components such as door inner panels of a car which are thick near the hinges and thin near the lock to withstand different types of loads or corrosion attacks. They are lighter and often cheaper compared to the conventional sheets. Tailored Blanks are usually made from steel. However aluminum and other dissimilar material TWBs are also available but less common.

Nowadays, TWBs are very popular in the industry, especially in automotive applications, due to demand of the reduced weight and longer service life of the component, and competition among the various industries has been increased. These industries compete in terms of technological innovation to gain the trust and confidence of the customers. Although, automotive products have their own specifications and

features, customers demand more in terms of fuel efficiency, performance, safety, and comfort at the cheapest price.

A TWB consists of two or more sheets that have been welded together prior to forming. The sheets may have either different shape, size, thicknesses or mechanical properties, which can be joined by various welding processes **(Merklein et. al. 2014)**. The weight of the part could be reduced while the strength of the part is maintained. Different body parts of a car made by TWB are shown in the figure 1.1.

This tailoring concept allows the engineer to join the best materials where necessary at the best place according to the material properties within the part. TWBs are popular among automotive applications because the weight of the component in a vehicle is crucial factor for the fuel efficiency and the TWB's is a solution for that due to the reduced weight of the part while maintaining the same strength.

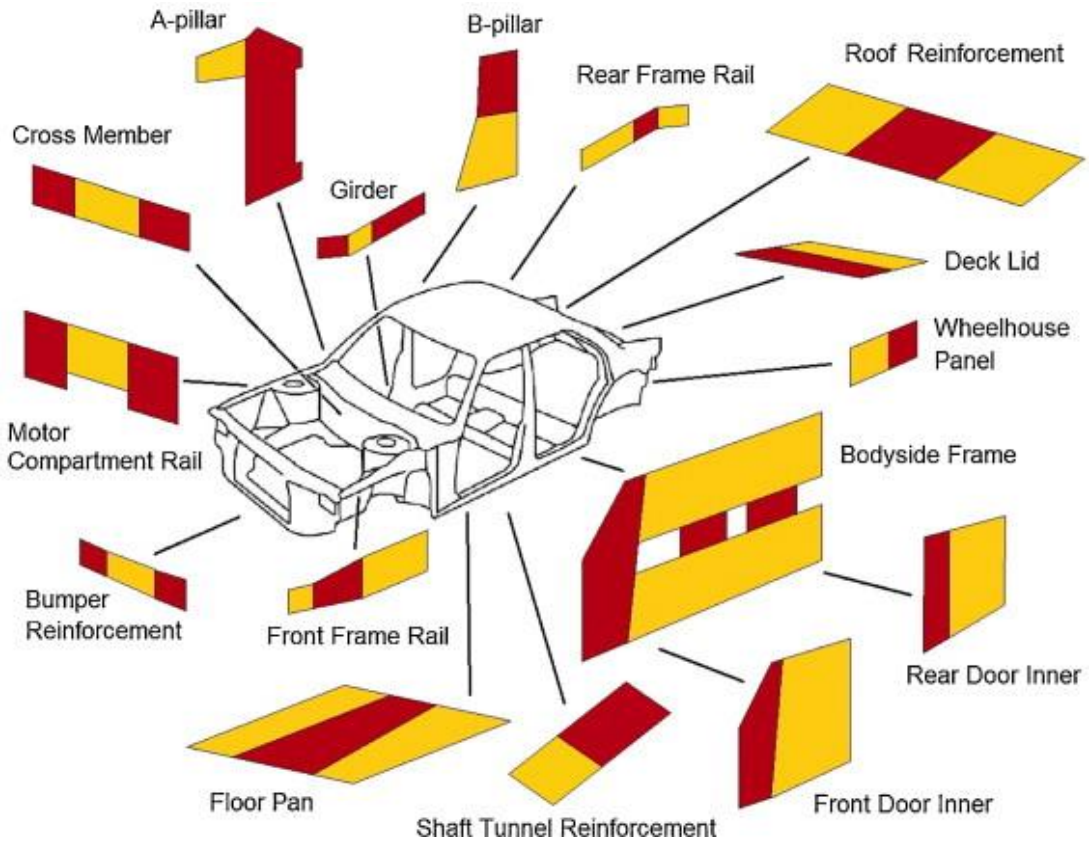

Fig.1.1: Different body parts of a car made by TWB. **[1]**

Higher strength material is used in the critical regions, while lower strength material is used in the less critical regions. This could significantly reduce the weight of the component and this concept is very useful in automotive applications. Luo showed that no material other than steel has shown the versatility in automotive applications.

TWBs were commercialized in around 1985 for a reinforced sun-roof and a cowl inner, with the same steel sheets joined together, for the improvement of material yield, auto body accuracy by reducing the number of panels, and productivity **(Zad 2010)**. Later in 1990, a front-side member was manufactured using TWB joined steel sheets with different grade. This prompted a new stage of development with a strong consciousness of improving automotive component performances including the improvement of crash worthiness by the optimal distribution of material by proper arrangement of sheet thickness and steel grade.

Various new grades of steel, interstitial-free steel (IF), dual phase steel (DP) and high strength low alloy steel (HSLA) have been developed which shows excellent formability and the ability to meet most automotive requirements to fulfil the demand of reduction in weight while maintaining the same strength. These newly developed grades of steel have flourished the TWB market alongside raising challenges which include the prediction and evaluation of the performance of these TWBs in forming, determination of residual stresses generated during welding and their other structural properties before and after forming. Therefore, it is essential to determine the deformation pattern and characterization of residual stresses within the component which evolve due to the presence of weld zone and different thickness combinations of the blank which affect forming behavior of tailor-welded blanks significantly. A good knowledge of variation, nature and magnitude of the residual stresses and of its distribution within the component is of great importance for the accurate assessment and evaluation of fatigue life of cold formed components.

Many methods could be used to analyze the results, among them the numerical method. Finite element modeling and numerical analysis is a well-known predictor of the deformation pattern and variation of residual stress when the forces and material properties are accurate.

1.2 Different types of Tailoring done for blanks

- Tailor Welded Blanks (TWB) are different sheets of metal welded together in the butt joint configuration.
- Tailored Strips are continuously welded strips.
- Tailored Coils are continuously welded coils of metals.
- Tailor Rolled Blanks (TRB) are metal sheets having continuously variable thickness. These different blank thicknesses are made on a cold rolling mill.
- Tailored Tubes (TT) are tubular components with thickness or strength variations, e.g. to be used in hydroforming.
- Tailored Orbitals (TO) are doughnut shaped whose ends are welded face to face for various automotive and industrial applications.
- Tailor Heat Treated Blank is a new development in this category, basically they are sheets that exhibit locally different material properties by local heat treatment which is used to change the properties of the material that show precipitation hardening such as steel, aluminum and their alloys etc. With this technology, the material properties can be optimized for subsequent deep drawing operations or for the final industrial application.

1.3 Advantages of TWBs

Reduced Weight

- By utilizing the appropriate material in the appropriate area, part weight can be reduced.
- Optimized distribution of material result in reduction of material use and hence, less scrap is produced.
- Gain in weight for the complete assembly.

Cost Reduction

- TWBs offer a significant cost saving due to reduced manufacturing costs and improved material utilization.
- By using expensive materials only where necessary, parts can be produced at a reduced cost.

Increase the technical performances without increasing the weight:

- Higher stiffness
- Better energy absorption
- Improved corrosion resistance
- Improved crashworthiness and part stiffness
- Improved dimensional accuracy and consistency

1.4 Limitations of TWBs

Decreased formability

Due to the welding of TWBs, the mechanical properties of the material will be changed and it might affect the formability of the TWBs. In particular, the potential elongation prior to tearing failure is significantly reduced.

Weld line movement

- Weld line movement creates several serious concerns in TWBs. First, the deformation concentration in the weaker material or thinner sheet may cause tearing failure due to the excessive strain created and simultaneous restricted elongation in the HAZ, particularly for aluminum TWBs.
- In addition to this, the weld line movement combined with a step in the fusion zone to accommodate the varying thickness of the TWB may cause a tearing failure concern if the step prevents the movement of the weld line.
- Finally, weld line movement restricted the ability of the automotive designer to position the material properties in the stamping or forming process where they are actually desirable.

1.5 The Future of Automobile Skin Panels: Tailor Welded Blanks

In 1999, tailor-welded blanks were still an innovation — the cutting edge of automobile. Olympic Laser Processing was a frontrunner with this technology with its facility that laser welds blanks in Van Buren Township, MI. Shortly, steelmakers and processors were linking up to serve the auto industry's growing preference for laser-welded blanks.

Since then, technology and demand have driven these new operations into a distinct industry segment here, in Europe, and in the Pacific Rim. Recently, Japan's JFE Steel purchased a $4.5 million welding line to keep up with the budding segment.

Automakers are using tailor-welded blanks to make cars safer, lighter, cheaper and more environmentally efficient; tailored blanks have become the future of automobile.

Tailor-welded blanks of steel are sheets of different thicknesses and grades, laser welded into a single flat blank prior to forming process to achieve the optimal material distribution and arrangement which further results in reduction in weight for cars, and to increase process efficiency and machine flexibility. Vehicle weight savings, part-count reduction, an improved stiffness/weight ratio, enhanced crash energy management, longer service life of component and an overall reduction in manufacturing costs are the results. With this manufacturing concept, automakers can add strength to parts where it is required and reduce a vehicle's overall weight and cost while maintaining the same strength.

Bob Lewinski, V.P., marketing and sales for VIL/Wayne Trail Technologies, explained the advantages of tailor-welded blanks. "It may be desirable to form a component such as an inner door panel that has a deep-draw depth to accommodate the contour of the finished vehicle door. This requires a very soft, and relatively thin metal. However, the front of the same inner door where the hinges will attach have to be strong enough to hold up the weight of the entire door. In the past, this would have required the

addition of several extra parts to strengthen this area. By producing a tailored welded blank with a large and thin piece of flat soft material joined to a thick and small piece of flat stronger material, this customized blank can then be formed into one piece inner door, deeply drawn in one area. He explained that using these blanks produces other tangible savings including reductions in scrap and weight, and improves dimensional accuracy by limiting use of higher-strength, heavier-gauge and more expensive materials.

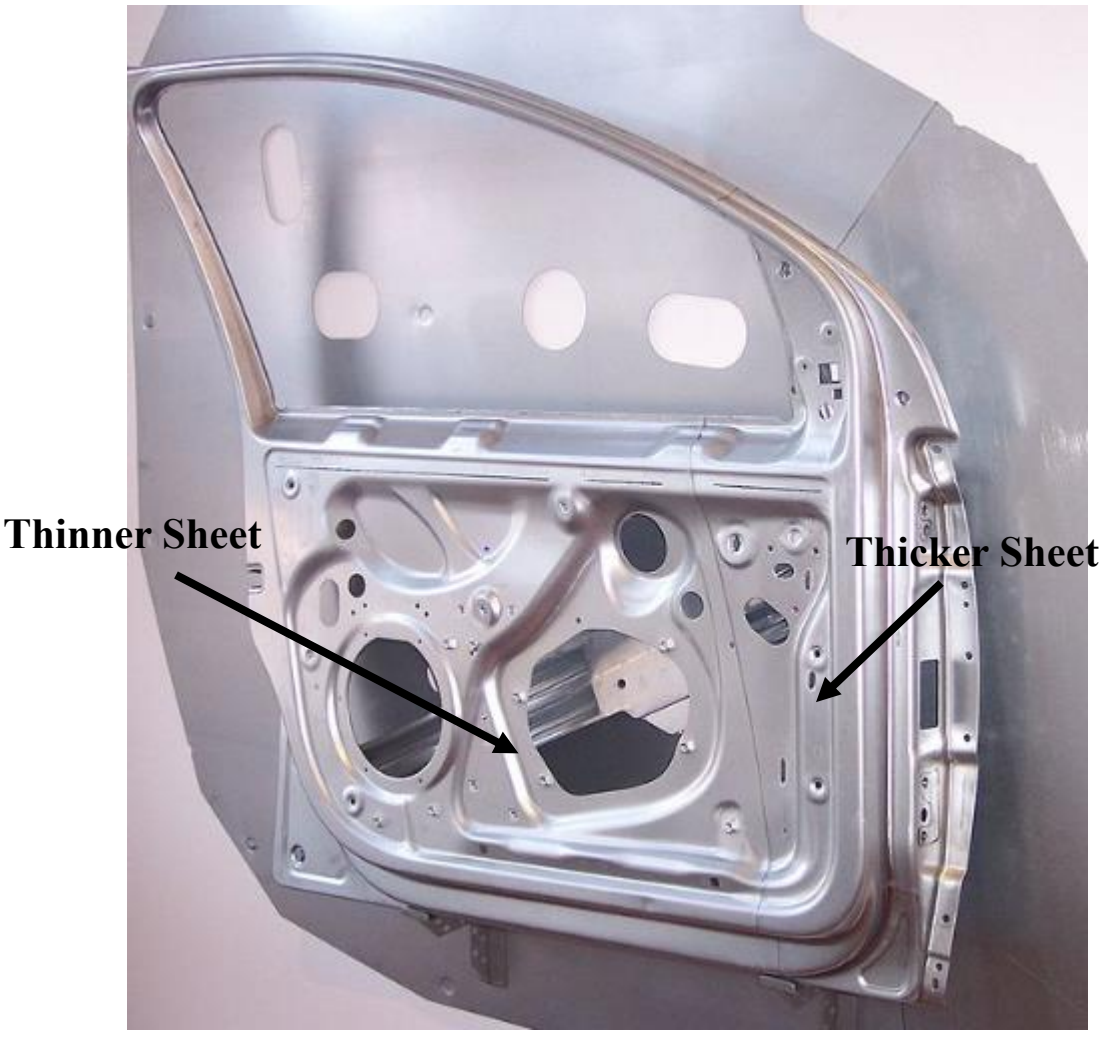

Fig.1.2: A lightweight door inner panel made by using TWB **(Stahlkocher 2006)**

1.6 Residual Stress

Residual Stress is “stress” inside of solid material that remains after the original cause of stresses (example, external forces, and heat gradient) has been removed. These stresses are locked-in stresses in the material that is free of external forces and thermal gradients. These stresses self-equilibrate within the cross-section of the material and can result in unexpected failure if not accounted for.

Residual stresses can also be defined as locked-in stresses remain inside a body in the absence of any cause of external loading or thermal gradients. In other words these stresses in a structural material or component are those stresses which exist within the object without the application of any service or other external loads. These stresses are may be tensile or compressive in nature.

1.6.1 Causes of residual stress

Residual stresses are unavoidable and these stresses can be present in any mechanical structure or component because of various factors. Manufacturing processes are the most common and frequent causes of generating residual stress in any component. Almost all manufacturing and fabricating processes such as casting, welding, machining, molding, heat treatment, plastic deformation during bending, rolling or forging introduces the residual stresses into the manufactured structure or component.

Residual stress could also be generated by localized yielding of the material, because of the sharp notches or from certain surface treatment processes like nitriding, surface hardening, quenching etc. Among the various factors that are known to cause residual stresses, basically are the development of deformation gradients in various sections of the piece by the result of thermal gradients, volumetric changes arising during solidification or from solid state transformations, and from differences in the coefficient of thermal expansion in pieces made from different materials.

1.6.2 Effects of residual stress

Residual stresses, depending on their nature, magnitude and distribution within the component, are either beneficial or detrimental. Residual stresses affects the performance of materials or components in a very significant manner. Fatigue, stress corrosion cracking, failures, distortion, structural stability are some of the common effects. Residual stresses often cause costly hidden problems whose effects will be seen during the service life of the components.

Depending on the nature of residual stresses, if these stresses are of sufficient magnitude and if they are tensile in nature they will accelerate certain failure mechanisms and hence, they become detrimental. These forms of failure include “pure” mechanical fatigue (that is without a significant corrosion effect), corrosion fatigue, hydrogen embrittlement (HE) and stress-corrosion cracking (SCC). Tensile residual stresses can be generated by a variety of manufacturing processes such as severe cold working, forging, casting, machining, grinding and electroplating. They may also be generated during the service period of the component due to thermal growth and contraction.

By contrast, compressive residual surface stresses as created by shot peening, cold rolling or by case hardening processes such as carburizing or nitriding are beneficial. They protect the metal against failures that typically initiate at the metal surface, e.g., any variety of fatigue or SCC. HE originates further below the metal surface and its control generally does not benefit from surface compressive residual stresses.

1.6.3 Relief of residual stresses

In general, residual stresses are unavoidable. However, it is possible to measure or control them to avoid their unwanted results. It is also possible to introduce these stresses intentionally in suitable amount with suitable processes to counter the detrimental effect of already existing residual stresses. Several methods which are used frequently for the relief of residual stresses are shot peening, laser peening, low plasticity burnishing and auto-frettage to extend the fatigue life of the critical components such as turbine blades, gear teeth, common rails etc.

The most effective way to control and analyze the residual stresses is to measure them. There are different methods available to measure these stresses. The commonly used methods are hole-drilling, X-ray diffraction, neutron diffraction, contour, slitting, ring core, deep hole drilling, etc.

Also there are several mechanical and thermal methods available to relieve the existing harmful stresses such as stress relief heat treatment, cryogenic treatment and vibratory stress relief.

1.6.4 Mechanical Methods

Mechanical methods usually aim to induce new compressive residual stresses to balance the detrimental effects of already existing tensile residual stresses. Mechanical methods consist of three different processes.

- **Peening processes:** Peening processes such as shot peening and laser peening are the two most common and easy cold working processes to induce compressive residual stresses. During shot peening the surface of a component is peened or stroked with small spherical balls, called shots. The peened action of the balls induces plastic deformation on the surface of the component, and hence, releases surface tensile stresses and introduces beneficial compressive residual stresses. During laser peening process, the surface of the component is peened with shock waves at high speed and high power which causes plastic deformation by yielding the material.

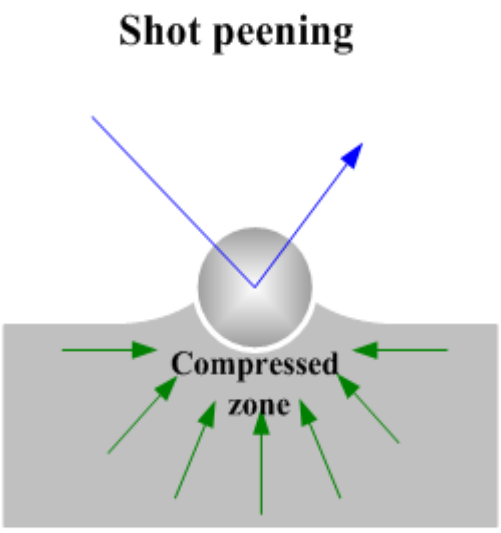

Fig.1.3: Shot peening process. **[29]**

- **Proof stressing:** As a stress releasing operation, proof stressing also plays a major role in testing of structural integrity of the component. During this process, a uniform load is applied to the component to reduce the already existing residual stress, by balancing the stresses by introducing new stress distribution.
- **Vibratory stress relief:** During this process, the component is vibrated at its natural frequency for a certain period of time to relive the already existing stresses within the component. Vibratory stress relief process is mainly used for dimensional stability of welded parts.

1.6.5 Thermal Methods

Thermal methods are generally a more common way to release the residual stresses than mechanical methods. Thermal methods usually do not induce any new stresses unlikely to mechanical methods to balance the adverse effects of already existing residual stresses inside the component. Thermal treatments can be separated into two categories as preheating and post heating treatments.

(a) **Preheating** is the thermal method which involves heating the component to increase its temperature to a higher degree than the room temperature and to a close degree to the process temperature. The degree of the temperature depends on the material

and the process. Preheating can be made in a furnace, with an induction coil or with hot blast.

If the temperature is lower than austenite formation range, the preheating treatment does not cause any dramatic changes in the microstructure because before austenite range iron only losses its magnetic character else there is no significant change in the properties of the material. When the temperatures are too high, recrystallization might occur which changes the microstructure. High temperatures may also cause surface oxidation, especially in stainless steels, where corrosion is possible. The preheated material will have better thermal gradients which cause a more uniform rate of heat transfer or cooling, but this may also cause a faster cooling rate which could soften the material.

b) **Post heating:** Post heating is the thermal method which involves heating the component to a temperature level which is the same or higher than the preheating temperature. Post heating is a stress relieving operation which aims to redistribute the residual stresses. Post heating does not have a standard which can be applied to all materials. Post heating parameters depend on the material and the size of the component. The cooling rates are again important for stress relieving.

1.7 Residual stresses due to welding

During the welding of TWBs, the weld area is heated up extensively compared to the surrounding area (HAZ and base metal), and fused locally. The material expands as a result of being heated up extensively. The heat expansion is restricted by the surrounding (colder) area, which gives rise to (elastic) thermal stresses **(Radaj, D.1992)**. These thermal stresses partly exceed the yield strength of the material, which is lowered at elevated temperatures due to refinement of grains.

Consequently, the weld area or the fusion zone become plastically hot-compressed due to the excessive heating and, after cooling down it become too short, too narrow or too small compared to the surrounding area. Thus weld area displays tensile residual stresses and the surrounding area (HAZ and base metal) displays the compressive residual stresses. Microstructural transformation during cooling involves an increase in volume. If this occurs at a (lower) temperature at which the yield strength is sufficiently

high, this results in compressive residual stresses in the weld area and tensile residual stresses generates in the surrounding area.

The generalized rule of thumb which applies to determine the nature of stresses in the areas of the component which have cooled down last, tensile stresses generate where thermal stress dominates, and compressive stresses generate where transformation or load stress dominates.

1.7.1 Residual Stresses in Tailor Weld Blanks

A Tailor Weld Blank is a flat sheet made by joining different pieces of metal either of similar or dissimilar materials having different shape, size and thicknesses. The presence of weld zone and different thickness combinations results in generation of residual stress in the blank which affect forming behavior of tailor-welded blanks significantly. Tailor Weld Blanks (TWB) has been used extensively in the automotive applications with the advantage of weight reduction whereas the Laser Beam Welding (LBW) process is widely used welding process for the joining of TWBs due to its faster rate of production with less amount of distortion **(Fonesca et. al 2016)**. Similarly, other welding process, such as Plasma Arc Welding (PAW) also use for the joining of TWBs, is characterized by a greater energy concentration and current density and therefore it results in lower distortion, higher penetration and higher welding speeds.

However, conventional welding processes such as gas welding, arc welding, resistance welding etc. have been studied extensively regarding the generation of residual stresses, but there are very less studies found about the characterization and analysis of residual stresses for the LBW and PAW joints. Therefore, it is important to analyze the residual stresses resulting from LBW and PAW processes by any residual stress measuring method e.g. X-ray diffraction technique with both $\sin 2\psi$ and $\cos\alpha$ method, Neutron diffraction technique in TWB butt joints.

Residual stress are internal forces acting within the body after removal of the external forces. As constraint stresses, they are in equilibrium only with themselves. However, reaction stresses originating from self-equilibrating support forces may superimpose on the constraint stresses. The total residual stresses superimpose on the

stresses generated from external load, i.e. the load stresses. Residual stresses may act either temporarily or permanently.

1.7.2 Longitudinal Residual Stresses along the weld line

Weld-longitudinal residual stresses arise as a result of the longitudinal contraction of the weld as it cools down, in certain cases superimposed by opposing transformation processes **(Radaj, D.1992)**. The different distributions presented in figures can be observed. The basis of the presentation is a plate strip with centric longitudinal weld treated as a plane model. In mild and low-alloy steel, the simple distribution occurs with high tensile stresses (reaching the yield limit) in the weld and lower compressive stresses alongside to it (the W shape) (Fig.1.4a). Such a distribution also occurs in the case of titanium, whereby the maximum stress is usually somewhat below the yield limit.

In aluminum alloys, the maximum stress is likewise below the yield limit, but with a slight superimposed trough in the weld (Fig.1.4b). In high-alloy steels with ferritic weld metal, the stress in the weld center is displaced into the compression range (the M shape) as a consequence of the austenite-ferrite transformation at low temperature (Fig.1.4c).

If, on the other hand, an austenitic electrode is used, the yield limit of the weld metal is reached in the weld. A compressive stress trough occurs to the right and left of that in the heat-affected zone, caused by transformation of the base metal after heating above the transformation temperature Acl the outside, the relatively high yield limit of the base metal is reached as a consequence of heating to below Ac1 (Fig.1.4d). Even further to the Outside, an additional reversal into the low tension range may occur as a consequence of the complex formation mechanism of residual stresses.

The zones of particularly high ensile stresses prone to cold cracking occur in or close to the weld in accordance with the basic presentation of figures depending on base and filler metal combination and various welding process parameters.

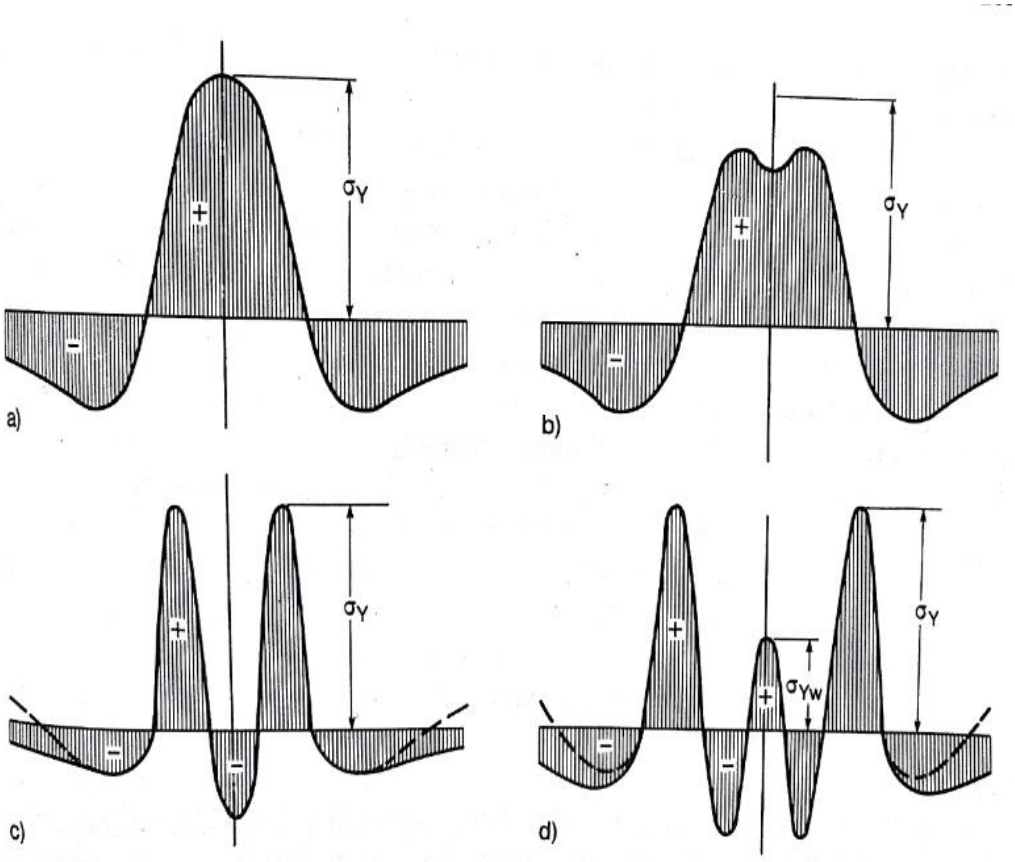

Fig.1.4: Weld longitudinal residual stress, stress profile variants: (a) mild steel, (b) aluminum alloy, (c) high alloy structural steel with ferritic and (d) austenitic filler material**. [21]**

1.7.3 Transverse residual stress across the weld line

Weld-transverse residual stresses arise directly as a result of the transverse contraction of the weld as it cools down, and indirectly as a result of longitudinal contraction, In addition, the different cooling processes on the surface and in the interior as well as possible superimposed transformation processes are influencing factors. The groove gap opening or closing, which can be observed experimentally, takes place primarily at high temperature with a correspondingly low yield limit, so that it has scarcely any influence on residual stresses **(Radaj, D.1992)**.

Transverse residual stresses at the butt weld in plates with unrestrained edges are primarily caused by restrained longitudinal contraction. Weld deposited immediately between two plates produces gaping in the middle section of the weld length if the weld

cools down without transverse restraint (Fig.1.5a). Accordingly, if the weld cools down transversely connected, transverse compression arises at the weld ends with a change to transverse tension when approaching the middle section of the weld length. The distribution which results for short plates is shown in figure 1.5b. A weld produced with slowly moving source, by contrast, results in high transverse tension at the weld end, thereby possibly causing incipient cracking (Fig. 1.5c). The above transverse stresses which are constant over the plate thickness are superimposed by transverse stresses varying over the plate thickness (compression on the surface, tension in the interior) which result from different cooling conditions on the surface and in the interior (Fig.1.5e).

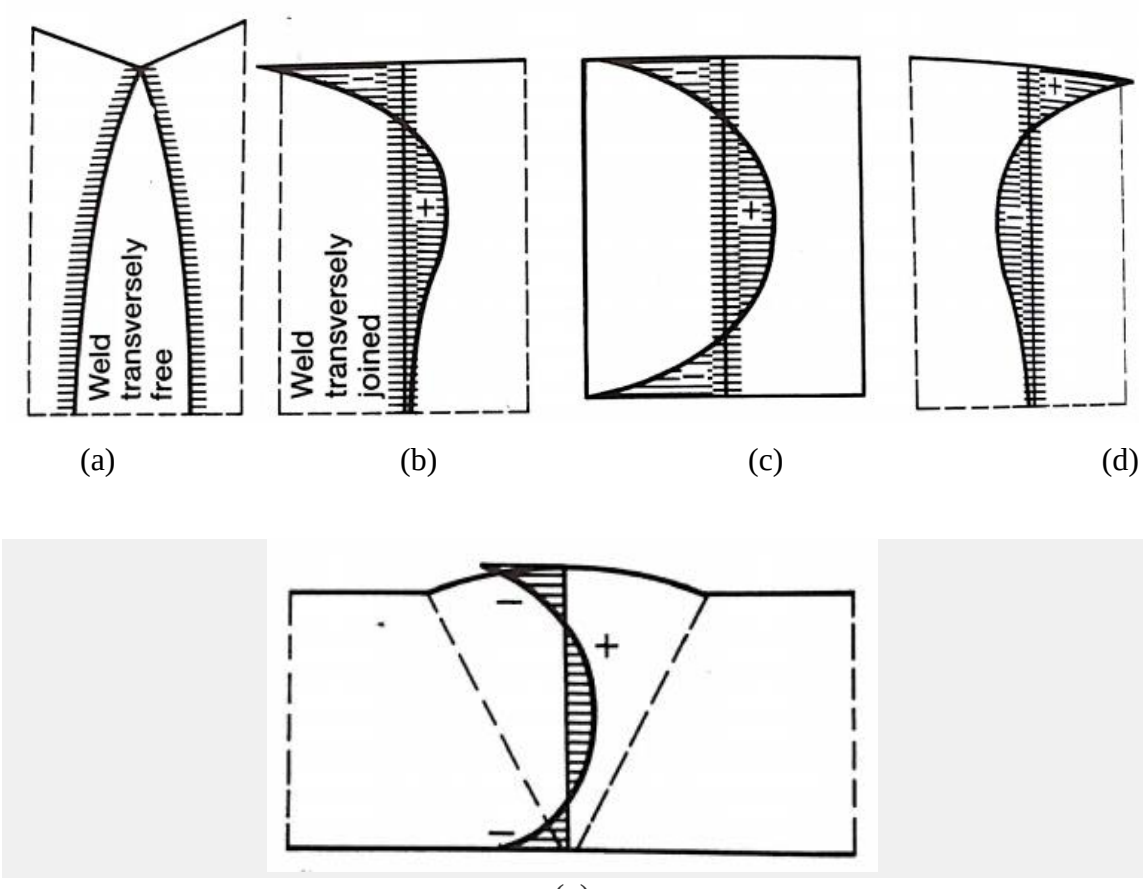

Fig.1.5: Weld transverse residual stresses: (a) rapidly deposited in long plate and (b) short plate, (c) slowly deposited in long plate (d) residual stresses over thickness to be superimposed (e) with V groove butt weld. **[21]**

1.8 Determination of Residual Stress

Residual stresses are the stresses which exist within a component or structure in the absence of any external forces, or it can be defined as the stresses which remains inside a body which is either stationary or at equilibrium with its surroundings **(Withers et. al 2001).** These stresses can be beneficial or detrimental depending upon its nature, to the performance and the life of a component. However, beneficial residual stresses can be introduced intentionally to nullify the detrimental effect of already existing stresses. It is really a very difficult and complex task to predict the residual stresses than the in-service or load stresses on which they superimpose, for this reason, it is very important to have reliable, accurate, precise and faster methods for the measurement of residual stresses.

Presently, there are a large number of methods available that can be used for the measurement of residual stress, these are destructive and non-destructive methods. Destructive methods are hole drilling method, crack compliance method etc. while non-destructive methods are X-ray diffraction, neutron diffraction etc. can be used without causing any significant destruction to the component; some have excellent spatial resolution, whereas others are restricted to near surface stresses or to the certain specific classes of material. In the case of destructive methods, a distinction requires to be made between complete and partial destruction of the component. The latter include small holes or ring grooves in the surface of the component, which permit further use of the part.

1.8.1 Destructive Methods

Destructive methods are used to determine the residual stresses in a wide range of engineering components. While seemingly less attractive than the non-destructive methods because of the specimen damage and hence the loss of material they cause and the amount of time they consume, the non-destructive methods are preferred over them because of their versatility, less time consuming process and reliability. Many different destructive methods and their variations have been developed to examine various component geometries and measurement objectives. Earlier, only components with simple geometries could be examined, now the availability of sophisticated computational tools and of high-precision machining and measurement processes have

greatly expanded the scope of the destructive methods for residual stress evaluation of the complex and intricate component geometries as well.

The crack compliance method **(Withers et. al 2001)** involves cutting a small slot in the component to examine the release of stress in the vicinity of the crack using strain gauge interferometry. By gradually increasing the depth of the slot, it is possible to resolve the stress field normal to the crack as a function of depth for relatively simple stress distributions. Material can also be removed chemically. A variant of this method has been used to assess the residual stress state of arteries in rabbits.

The hole drilling method **(Withers et. al 2001)** in which undisturbed regions of a sample containing residual stresses will transform into a different shape when the locality is machined, thereby providing data for the back-calculation of residual stress. The machining operation usually involves drilling a small hole around which the strain is measured by using either combination of strain rosettes in three independent directions, laser interferometry based on a rosette of indentations or holography. Although it is possible to deduce the variation in stress with depth by incrementally deepening the hole, it is difficult to obtain reliable measurements much beyond a depth equal to the diameter. With an arrangement of three strain gauge rosettes, it is only possible to measure the two in-plane components of the stress field. Nevertheless, this method is cheap, widely used and it has been applied even to polymeric samples.

1.8.2 Non-destructive Methods

Residual stresses or strains are measured non-destructively by means of the X-ray method **(Radaj, D.1992)**. X-rays are diffracted crystal lattices and produce interference phenomena, from which it is possible to draw conclusions relating to the inter-planar spacing of the lattice. The load stress or residual stress is determined from the change in the inter-planar spacing compared to the stress-free state. The reflection method is used in practice. An X-ray striking the surface of the component produces, after reflection, interferences which appear on a slewed film (according to Debye-Scherrer) as an interference ring. More modern equipment uses a scintillation counter instead of the film.

Two different techniques $\mathbf{sin^2\,\Psi}$ and **cosα** can be used with X-ray diffraction method to measure the residual stresses.

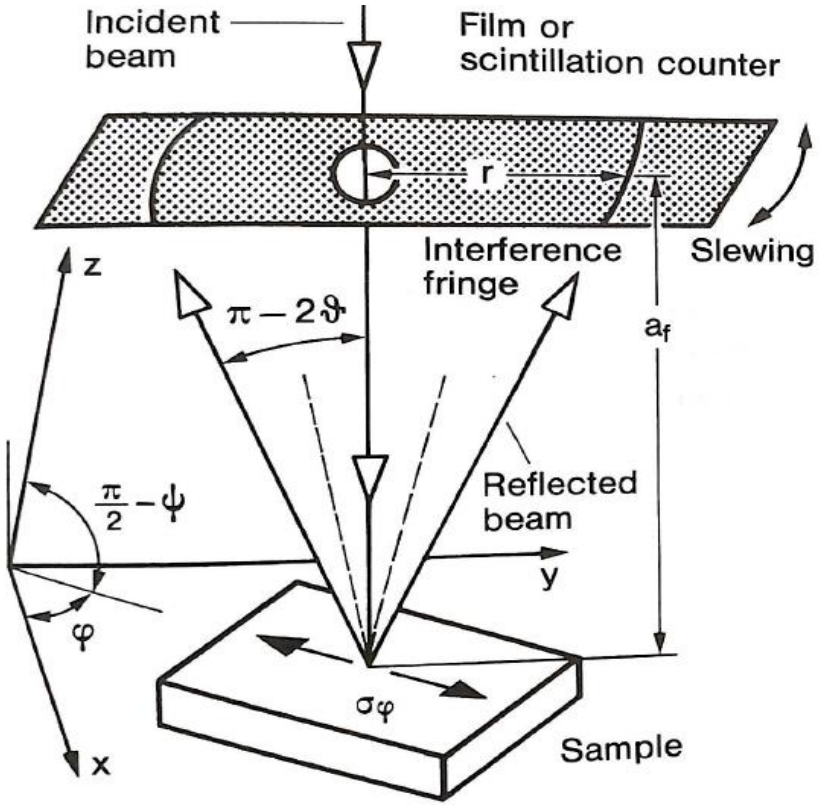

Fig.1.6: Residual stress measurement by X-ray reflection method **[21]**

The Interference line, of the first order, satisfies Bragg's law (with n=1), to which the glancing angle depends on the inter-planar spacing CIA of in the crystal lattice and on the wavelength of the X-radiation.

$$2d \sin \theta = n\lambda$$

Where d is inter-planar spacing, θ is angle of incidence and λ is wavelength of x-ray.

Another more recently developed non-destructive stress or strain measuring technique is the neutron diffraction method **(Radaj, D.1992)**. Neutrons are scattered by the atomic nuclei, whereas X-rays are scattered by the electron shells with the consequence that neutrons penetrate far deeper than X-rays, i.e. up to 3 cm in steel or 30 cm in aluminum alloys.

Thus stresses or strains can be measured in the interior of the component. Typically, a neutron beam from the reactor core (approx. 50 x 50 mm2) is transmitted by a monochromatic crystal, Slits in absorbing cadmium masks are placed between the component and both the incident and the diffracted beam in order to reduce the sampled volume of residual stress (Fig.1.7). Parallel scattered beams originate from the crystallographic planes which have the correct orientation for diffraction.

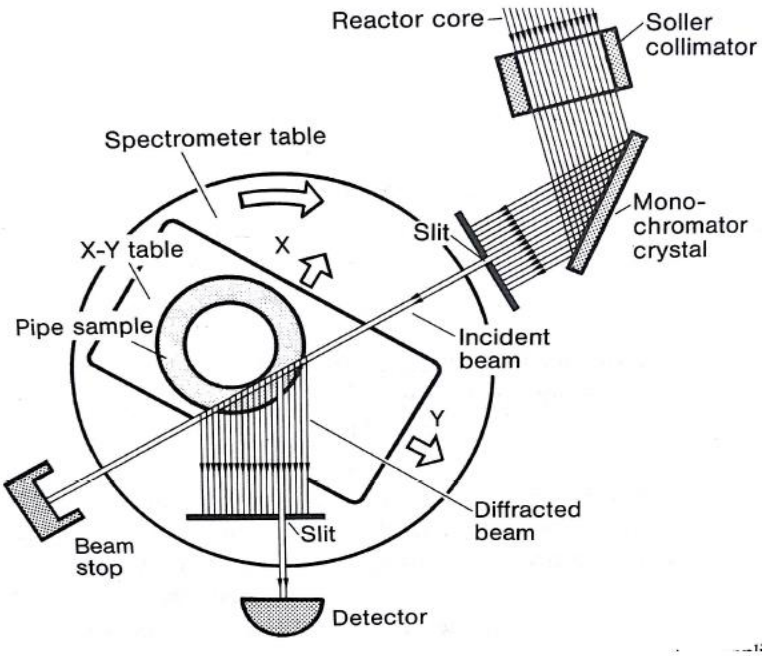

Fig.1.7: Residual stress measurement based on Newton Diffraction. **[21]**

Electron diffraction **(Withers et. al 2001)**, a non-destructive method in which very high lateral spatial resolution can be achieved by using electron beam which can readily be focused to diameters as small as 10 nm. The convergent beam electron diffraction technique is commonly used to obtain the greatest strain resolution. Very thin samples, diameter less than 100 nm can also be examined by this method, which naturally renders the results vulnerable to surface relaxation effects and the strain values represent an integral through the thickness. Also, this method provides a way of measuring few very typical stresses, such as the misfit strains between γ/γ' phases in nickel super-alloys and 'macro-stresses' in very small electronic device structures.

In Ultrasonic measurement **(Withers et. al 2001)**, changes in ultrasonic speed of the wave can be observed when a material or component is subjected to stresses, the changes providing a measure of the stress averaged along the wave path. The acoustoelastic coefficients necessary for the analysis are usually calculated using calibration tests for the each sample of the different material being examined. Different types of wave can be employed for the evaluation of stresses, but the commonly used technique is the critically refracted longitudinal wave method. The greatest sensitivity is obtained when the wave propagates in the same direction as the stress.

This method provides a measure of the macro-stresses over large volumes of material. Ultrasonic wave velocities can depend on microstructural inhomogeneities, and there are difficulties in separating the effects of multiaxial stresses. Nevertheless, being portable and cheap to undertake, the method is well suited to routine inspection procedures and industrial studies of large components, such as steam turbine discs.

CHAPTER 2

LITERATURE REVIEW

2.1 Literature Review

Merklein M. et al. [1] reviewed the production, applications and evaluation on tailor weld blanks. Tailor weld blank is the collective for semi-finished sheet products which are characterized by variation of the sheet thickness, sheet material, coating or material properties. With these adoptions, the tailor weld blanks are optimized for a subsequent forming process. In principle four different approaches can be distinguished to realize tailor weld blanks: joining materials with different grade, thickness or coating by a welding process (tailor welded blanks), locally reinforcing the blank by adding a second blank (Patchwork blanks), creating a continuous variation of the sheet thickness via a rolling process (tailor rolled blanks) and adapting the material properties by a local heat treatment (tailor heat treated blanks). The major advantage of products made from tailor weld blanks in comparison to conventional products is a weight reduction. This study covers the state of the art in scientific research concerning tailor weld blanks. The review presents the potentials of the technology and chances for further scientific investigations.

Kinsey B. [2] illustrate the significance of tailor welded blanks for the automotive industry. One of the extensive users of sheet metal components capitalizing on the advantages of tailor welded blanks (TWBs) is the automotive industry. These advantages include reductions in weight, cost and noise with simultaneous increases in crashworthiness, dimensional accuracy and corrosion resistance. However, there are formability concerns that are present due to the welding process. In this study, these advantages and disadvantages are discussed along with TWB forming methods, welding processes and materials used in the automotive industry.

Anand D. et al. [3] studied the fatigue behavior of tailor (laser)-welded blanks for automotive applications. The aim towards reduction of weight in the automotive industry has led to the evolution of tailor-welded blanks (TWBs) for structural applications. This work significantly aimed at evaluating the fatigue behavior of the TWB's having different thickness combinations and compositions with and without zinc coating. The results showed that TWBs made from zinc-coated/galvanized steels exhibited a lower fatigue limit as compared with the TWB combination from uncoated bare metals. This was attributed to the intergranular cracking in the galvanized TWBs caused by the presence of zinc penetrating under the sheet surface. The fracture surface of the uncoated TWB was basically characterized by the fatigue striations.

Fengxiang X. et al. [4] study shows the experimental investigation on high strength steel (HSS) tailor-welded blanks (TWBs). This study aims to investigate mechanical characteristics of the tailor-welded blank (TWB) components made of high strength steel (HSS). A series of HSS-TWB plates with different orientations of weld line are studied through three-point bending test to evaluate the effects of different design parameters such as weld line location, on the deformation behaviors. The experimental results show good repeatability of tests and the relative shift phenomenon between indenter and specimen is observed and analyzed for the TWB steel sheets with different weld line orientations at parallel and 45◦ to the bending moment, respectively. The experimental results include the force vs displacement curves and some detailed photographical images throughout the loading process. It is found that the discrepancy of different combinations is quite noteworthy.

Song Y. et al. [5] studied the influences of thickness ratio of base sheets on formability of tailor welded blanks were examined based on Erichsen cupping tests. Three-dimensional finite element (FE) models were prepared using Hill’48 yield criterion and iso-hardening rule and ABAQUS software is used for the FE analysis. The failure onset sites of tailor welded blanks were analyzed and the quantitative relationships between the Erichsen index values and base thickness ratio were established. Based on these relationships, the formability of tailor welded blanks made from dissimilar base sheets are examined, provided that the Erichsen index values of tailor welded blanks made

from identical ones are known and that the above two different types of tailor welded blanks undergo a similar stamping process. The experiments were then carried out to validate this method.

Gautam V. et al. [6] illustrate the experimental and numerical investigations on springback in V-bending of tailor-welded blanks of interstitial free steel. The presence of weld zone, difference in thickness and high anisotropic behavior affect forming behavior of tailor-welded blanks significantly. Therefore, incorporation of anisotropy of the sheets nt66and properties of the weld zone in finite element simulations is very important for accurate prediction of springback in bending of tailor-welded blanks. In this study, experimental and finite element simulations of V-bending were carried out on tailor-welded blanks of three thickness combinations, prepared by Nd-YAG laser welding of interstitial free steel sheets of thicknesses 0.8, 1.2 and 1.5 mm. The orientation of the weld line in longitudinally welded blanks was kept at 0°, 45 °and 90° with respect to the rolling direction to study the effects of anisotropy on springback in V-bending. The tensile properties of the weld zone in different thickness combinations were determined and incorporated in finite element simulations for prediction of springback. It was observed that springback results were mainly governed by the springback behavior of the thicker sheet in a particular thickness combination. Weld zone properties affect the springback of tailor-welded blanks more significantly than the anisotropy of the sheets. Accuracy of predicted values of springback in simulations increased when the properties of the weld zone were incorporated in the material model.

Rojek J. et al. [7] has studied the methods for the determination of mechanical properties of the weld zone in tailor-welded blanks. Mechanical properties of the weld zone are necessary for accurate modeling of forming processes involving tailor-welded blanks (TWB). TWB's are usually produced by laser welding. Due to the small size of the weld cross-section, it is not possible to use standardized tests to determine the mechanical properties of the weld zone in tailor-welded blanks. Special testing procedures must be employed. This study presents different methods which can be used to determine mechanical properties of the weld zone in tailor-welded blanks. Methods based on experimental tests as well as those combining experimental procedures with

numerical studies are described. The presented methods include uniaxial tension tests, microhardness tests and indentation tests combined with inverse numerical analysis. The stress–strain relationships for the weld zone in a steel laser welded blank obtained using different methods have been compared with one another.

Fonseca M. et al. [8] study focused on the evaluation of residual stress and mechanical properties of TWBs welded by laser welding processes. They studied that tailor weld blanks (TWB) have an extensive application in the automotive industry where the Laser Beam Welding (LBW) process is widely used due to its high productivity. Similarly, the other used welding process, Plasma Arc Welding (PAW), is characterized by a greater energy concentration and current density and therefore lower distortion, higher welding speeds and higher penetration may be obtained. However, while the conventional welding processes have been extensively studied regarding the generation of residual stresses, there are few studies about residual stresses characterization and analysis of LBW and PAW joints. Therefore, the aim of the present work is to analyze the residual stresses resulting from LBW and PAW processes by X-ray diffraction technique with $\sin 2\psi$ method in TWB butt joints. For both joints, macro and microstructure were characterized and mechanical properties were determined. Tensile residual stresses in the heat-affected zone (HAZ) and in the fusion zone (FZ) were verified for both welding processes.

Now further focusing on the welding characteristics of the TWB's after welded by LBW or any other welding processes the presence and evaluation of the residual stress is the main problem. In recent **Thasanaraphan P. et al. [9]** studied the welding characteristics of Tailor Welded Blank metal sheets using GTAW and laser Welding process. To determine the thermal fields during the welding process, the equation of energy conservation is required. The heat transfer of laser beam welding is usually calculated by applying classical heat conduction theory. The thermal analysis is conducted using temperature dependent thermal material properties. In a thermal cycle, heating and cooling, thermal strains occur in the weld metal and base metal regions near the weld. The strains produced during welding are accompanied by plastic deformation.

The stresses resulting from these strains produce internal forces that cause bending, bucking, and rotation. It is these displacements that are called distortion.

Now stress behavior of TWB is measured after it welded by the laser welding process. A study is being done on the stress behavior of tailor-welded blanks for dissimilar metals using finite element method by **Rahman M. et al. [10]**. The stress behavior of tailor-welded blanks (TWBs) for dissimilar metals and identifies the critical locations using the finite element method. By using dissimilar metals with different welding configurations, the critical points where the force is concentrated and the maximum forces that are exerted at those particular points can be estimated.

Olabi A. et al. [11] study illustrate various non-destructive techniques are used in the measurement of residual stresses in TWB's are X-ray diffraction technique, neutron diffraction technique. A study is done on methods for measuring residual stresses in components. Residual stresses are one of the main factors determining the engineering properties of parts and structural components. This fact plays a significant role, for example, in fatigue of welded elements. Many different methods and variations of methods for measuring residual stresses have been developed to suit various specimen geometries and measurement objectives. The purpose of this study is to classify the different methods and to provide an overview of some of the recent advances in the area of residual stress measurement and act as a summary document to aid technique selection between destructive, semi-destructive and non-destructive techniques for residual stresses. For each method scope, physical limitation, advantages and disadvantages are summarized. In the end this study indicates some promising directions for future developments.

Now focusing on the non-destructive techniques a study is being done on the residual stress characterization of welds using X-Ray diffraction techniques by **Brauss M. et al. [12].** Neglect of residual stresses created during welding processes can lead to stress Corrosion cracking, distortion, fatigue cracking, premature failures in components, and instances of over design. Automated residual stress mapping and truly portable

equipment have now made the characterization of residual stresses using X-ray diffraction (XRD) practical. The non-destructive nature of the x-ray diffraction technique has made the residual stress characterization of the welded components a useful tool for process optimization and failure analysis, particularly since components can be measured before and after welding and post welding processes.

Another non-destructive technique is studied by the **International Atomic Energy Agency [13]** in 2005 is measurement of residual stress in materials using neutrons. Measurement of residual stress is an area where neutron diffraction has proved to be very significant and fruitful. It is possible to design a device for a neutron beam on a medium flux research reactor with appropriate parameters like beam intensity and resolution and components like detectors and collimators. The method has been used to measure and characterize residual stress distribution in critical components like large bearings of a crankshaft of the car, strain distribution in the cross-section of a rail wheel and rail welds. The deformations in these components at the microscopic level are very critical and could lead to severe accidents. The testing of reliability of a product or the diagnosis of the failure of a component could thus be done effectively.

Neutron scattering has played an important role in studying dynamics and structure of condensed matter. The special nature of neutron interaction with matter provides important complementary and supplementary data to other techniques. The location of hydrogen atoms in the presence of heavy elements, for example, can only be determined by means of neutron diffraction studies. Crystal structures of biological systems, like amino acids and polypeptides, have been elucidated using single-crystal neutron diffraction. The behavior of magnetic materials can also be explored for both scientific and industrial applications.

The large penetration depth and selective absorption of neutrons make them a powerful tool in NDT of materials. Residual stress formed in a material during manufacturing, welding, utilization or repairs can be measured by means of neutron diffraction. In fact neutron diffraction is the only NDT method, which can facilitate 3-D mapping of residual stress in a bulk component. Such studies can help to improve the manufacturing quality of engineering components and to optimize design criteria in

applications. Anisotropies in thermal and electrical conductivities, for instance of fuel elements, and mechanical properties of materials depend on the textures developed during their preparation or thermal treatment. Textures can be studied using neutron diffraction techniques, which are developed and used in many research reactors.

To overcome these issues, simulation using the finite element method is used to estimate the critical point of the TWBs. Steel and aluminum are considered as welding materials. The welding parameters of current, voltage and welding velocity are modified to analyze the effect on the welding part.

The different TWB configurations are the L-shape, the T-shape and the plate. Goldak's double ellipsoid source model is used as the heat source in the investigation. The distortion of the plate increases when the power of the laser increases. The distortion is due to the residual stress caused by heating when welding. The residual stress relieved during cooling makes the plate distort. It can be seen that the increase in power increases the temperature since power is the energy source conducting heat to the plate. Thus, the temperature is proportional to the power used. The heat-affected zone increases during the welding process when the power increases. Increasing the power also increases the TWB distortion.

Pineault J. et al. [14] focused on the Residual Stress Characterization of Welds Using X-Ray Diffraction Techniques. Neglect of residual stresses created during welding processes can lead to stress corrosion cracking, distortion, fatigue cracking, premature failures in components, and instances of over design. Automated residual stress mapping and truly portable equipment have now made the characterization of residual stresses using X-ray diffraction (XRD) practical. The characterization of the residual stress of welds by using x-ray diffraction technique due to its nondestructive nature has made it a useful tool for process optimization and failure analysis, particularly since components can be measured before and after welding and post welding processes. This study illustrates the significance of residual stress characterization in welds and presents examples where x-ray diffraction techniques were applied in the characterization of various kinds of welds including laser welds, arc welds, TIG welds, resistance welds and electron beam welds. Numerous destructive and non-destructive techniques are available

to manage potentially harmful residual stresses created during the welding process thus, the effects of a few example post weld processes such as grinding, heat treating and shot peening are also addressed.

Ling J. et al. [15] study elaborate on the characterization of a portable x-ray device for residual stress measurements. In this study, a thorough analysis of the operating parameters required to obtain reliable results from a portable X-ray residual stress analyzer utilizing an image plate detector is presented. In order to quantify the instrument precision and accuracy of the stress values, a series of measurements with stress-free ferrite powder and a solid platinum specimen were conducted using both the traditional sin^2Ψ and the "cos α" method. Results for the same samples by both methods are obtained by both methods and compared to quantify the instrument precision and accuracy of the stress values. Detailed measurement conditions for an accurate stress assessment are also reported.

Peterson N. et al. [16] shows the assessment and validation of cosα method for residual stress measurement. Traditionally, X-ray diffraction techniques have allowed for non-destructive testing of the material for qualification purposes by utilizing traditional stationary diffractometers. Recently, portable x-ray residuals stress analyzers have frequently been used due to the ease of use. The cosα technique has shown a faster method of measuring residual stresses incorporated in portable devices due to its ability to measure an entire Debye ring at once from the two-dimensional detector, thus not requiring multiple samples tilts as in case of sin^2Ψ method. In this study, shot-peened steel samples were subjected to residual stress measurement from both the cosα and sin^2Ψ technique using a portable device and laboratory diffractometer respectively.

Two different types of data analyses were performed to calculate the residual stresses based on linear regression and least-squares analysis. The results from these two analyses shows the equivalency in both accuracy and precision of the cosα to the traditional sin^2Ψ technique in measuring residual stresses in shot-peened materials. Based on these results, recommendations are presented on the use of X-ray diffraction analyzer based on cosα technique for residual stress measurement.

Clapham L. et al. [17] illustrate the residual stress mapping in same gauge and differential gauge tailor-welded blanks by using neutron diffraction technique which used to determine the residual stresses in the weld region of laser-welded tailor-welded blank (TWB) samples. Residual stresses in same gauge and differential gauge TWB samples are examined in the as-welded condition as well as after uniaxial loading to 0.5, 3.0 and 7.0% strain. This study significantly explains that the trend in the residual stress parallel to the weld is explained by considering that the shrinkage in the weld direction is constrained by the parent material during cooling of the fusion and heat affected zone. This results in residual tension developing in the weld direction near the fusion zone. This stress is balanced by compressive stresses away from the fusion zone. Results indicate that stress distributions can be quite complex, particularly following deformation. However, two major conclusions were drawn: first, residual stresses around laser welds in these TWBs tend to be small compared with stresses reported for conventional welding processes. Secondly, in most cases the peak residual stresses tend to remain the same or diminish with subsequent deformation.

Sasaki T. et al. [18] illustrate the influence of image processing conditions of Debye Scherrer ring images in x-ray stress measurement using an imaging plate. This describes the study of the possibility of X-ray stress measurement in which stresses are obtained by analyzing the whole of one diffraction ring detected with a two-dimensional X-ray detector called an imaging plate (IP). The theory of the stress determination proposed by Taira et al was shown and advanced to make measurable all plane stress components. The experiment showed good agreement with stresses applied mechanically.

2.2 Research Gaps

Residual stress presence in TWB's is a main concern because it affects their behavior significantly during forming processes. Especially presence of tensile residual stresses is detrimental because it leads to severe damages of the components. Hence their characterization and determination is necessary for the long service life of the component. In literature very less work is found regarding characterization and numerical analysis of residual stress due to springback after bending process of IF steel. As steel is used extensively in automotive sector and TWB's are preferred over conventional sheets due to the advantages of higher strength and lighter weight, it is really important to determine the nature and magnitude of residual stresses present in the blanks to avoid the failure of the component.

Several destructive and non-destructive methods are available for the experimental of residual stresses but very few studies have been found based on non-destructive X-ray diffraction method used for experimental determination of residual stresses in the blanks. Still there are few studies available which uses this method with $\sin^2\Psi$ technique for the calculation of stress after calculating the change in interplanar spacing d. But a new "cosα" technique has been developed for the easy and faster measurement of stresses by using X-ray diffraction method with a formation of 2D debye ring.

Hence, in this study "cosα" technique with X-ray diffraction method is used for the experimental determination of residual streses in TWB's of IF steel with thickness combination of 0.8 mm × 1.5 mm which is generated due to sprinback after bending with three different punch profile radius of 10mm, 12.5mm and 15mm to characterize the behavior of residual stress before and after springback and also to determine the variation of residual stresses with different punch profile radius for the constant thickness ratio.
Numerical analysis (FEA) is performed on the ABAQUS software, all three simulations for the different punch profile radius is being performed with introducing the various properties for the thin sheet, thicker sheet and weld zone. So that the experimental and numerical characterization of residual stress can be done and obtained results should help in avoiding the failure and hence, increasing the service life of the components.

2.3 Objectives of the study

The main objectives of this study are to characterization of the material for the tensile testing, anisotropy and determination of residual stresses in parent sheet and Tailor Welded Blanks of IF steel.

- To investigate the tensile behavior of IF steel specimens of thickness 0.8mm and 1.5mm and TWB with thickness combination of 0.8mm×1.5mm. To determine the anisotropy of the IF steel sheets.
- Characterization of nature of residual stress and determination of its magnitude using Pulstecc μ360 residual stress analyzer.
- Finite Element analysis of bending of TWB with thickness combination of 0.8mm×1.5mm and its springback simulation using ABAQUS software. Prediction of the magnitude of longitudinal stresses and residual stresses during bending and after springback respectively.
- Validation of the predicted results with the results obtained by experiments.

CHAPTER 3

METHODOLOGY

3.1 Selection of material

The automobile sector requires more steel options to meet increased demand of specifications for strength, part complexity, crash-worthiness, energy absorption, and dent resistance **(G. E. Opbroek 2009)**. To achieve these specifications, the international community of steel has developed a new category of steel known as Advanced High-Strength Steels (AHSS). Basically, AHSS consist two distinct families of steel based on their strength, the first is the high-strength steels (HSS) with increased formability of the steel for more complex and intricate part designs which includes dual phase (DP) and transformation induced plasticity (TRIP) steels. The second family of AHSS has increased tensile strength while maintaining good energy absorption and crush resistance ability, these are complex phase (CP) and martensitic (Mart) steels.

Increasing demand of safer and lighter vehicles will set the trends of the steel market for the design of various parts of future vehicles (**M. C. Theyssier 2015**). That is the reason why new generations of AHSS grades are already being studied extensively and even started new development in the steel market. These new generation steels will include higher percentage of alloying elements (from 8 to 10%, up to 20–30%) and results in some interesting properties such as lower density of the steel with a better combination of strength and formability, with improved performance against the crashes and the ability to make the vehicles lighter. Although, manufacturing challenges will, of course, be specific to those new developed grades of steel, irrespective of their final process: either hot or cold stamping or roll forming.

Automotive steels can be defined in three distinguished categories. The first category is based on the metallurgical designation of the steels, which includes low-strength steels (interstitial-free and mild steels); conventional high-strength steels (carbon-manganese, high-strength IF, and high strength, low-alloy steels); and the newer

types of advanced high-strength steels (dual phase, transformation induced plasticity, complex phase, and martensitic steels).

In second category steels are classified on the basis of their strengths which falls into the certain specified range. High-Strength Steels (HSS) are those steels whose tensile strengths falls in the range of 270–700 MPa , whereas Ultra-High-Strength Steels (UHSS) are steels with tensile strengths greater than 700 MPa.

A third classification category uses another mechanical property that is total elongation, a property related to formability of the material. Figure 3.1 compares total elongations for the different types of steel. As shown in the figure, the tensile strengths of AHSS overlap the range of both HSS and UHSS tensile strengths. In general, the AHSS category of steels has greater total elongations than conventional HSS of similar tensile strengths. Hence AHSS can be used to make the vehicles or complex parts of vehicles to maintain the same level of strength with lighter weight.

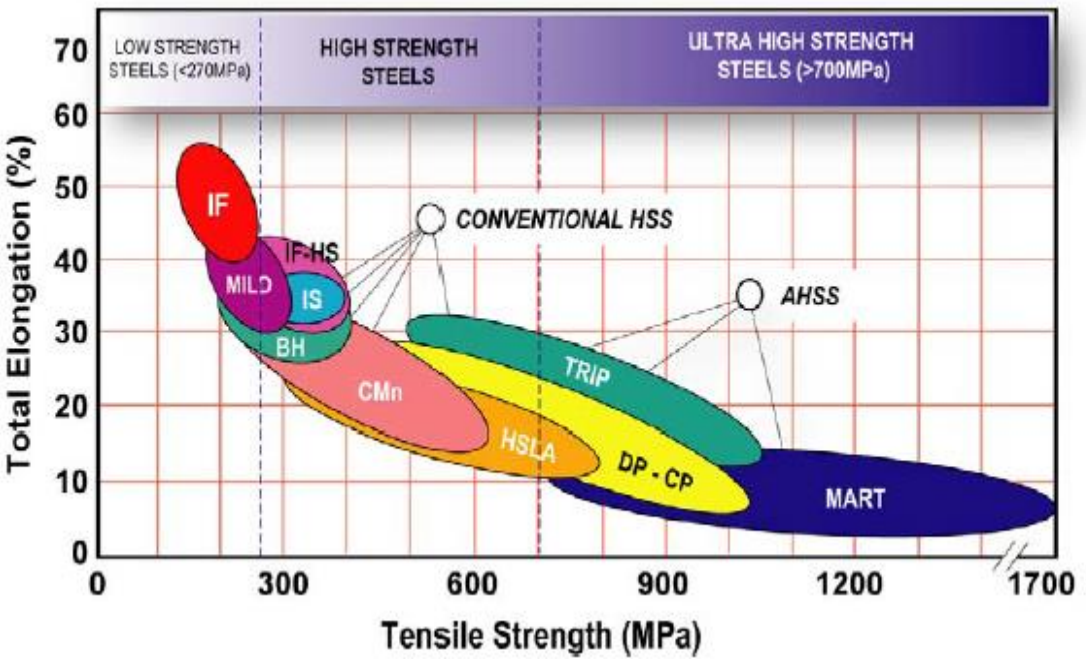

Fig.3.1: Strength-Elongation relationships for low strength, conventional HSS, and Advanced HSS steels. **[22]**

3.2 Metallurgy of AHSS

The fundamental metallurgy of conventional low and high-strength steels is generally well understood by manufacturers and consumers of various steel products. Whereas, the metallurgy and processing methods of various grades of AHSS are somewhat novel or excellent compared to conventional steels, they will be described here to provide a basic understanding of how their excellent mechanical properties evolve from their unique method of processing and structure with the addition of various alloying elements in the variable amount.

3.2.1 Dual Phase (DP) Steel

These steels consist of a ferrite matrix in which a hard martensitic second phase material present in the form of islands within the matrix. As shown in figure 3.2 a schematic microstructure of DP steel, which contains ferrite matrix with the islands of martensite present in it **(G. E. Opbroek 2009)**. The soft ferrite phase is generally continuous, which offer these steels excellent ductility, hence better formability is achieved. When these steels deform, strain is concentrated in the lower-strength (soft) ferrite phase surrounding the islands of martensite, creating the unique high work-hardening rate exhibited by these steels.

In DP steels, addition of carbon enables the formation of martensite (hardest constituent of Fe-C family) at practical cooling rates which results in increasing the hardenability of the steel. Manganese, nickel chromium, molybdenum, and vanadium, added individually or in combination to achieve certain desired properties and also helps in increasing hardenability, corrosion resistance and various other desirable properties of the steel. The addition of various alloying elements are balanced carefully, not only to produce unique mechanical properties, but also to maintain the generally good resistance spot welding capability.

3.2.2 Transformation-Induced Plasticity (TRIP) Steel

These steels consist of a matrix of ferrite as a primary constituent in which retained austenite embedded. In addition to retained austenite (minimum of 5% of volume), phases of hard constituent such as martensite and bainite are also present in varying amounts in the islands of ferrite matrix. During deformation, the dispersion of hard phases in soft ferrite creates a high work hardening rate, a similar phenomenon observed in the DP steels **(G. E. Opbroek 2009)**. However, in TRIP steels the retained austenite also progressively transforms into the martensite with the increasing strain, thereby increasing the work hardening rate at higher strain levels. A schematic of TRIP steel microstructure is shown in Figure 3.3.

TRIP steels contain carbon in higher quantities than DP steels to lower the martensite transforming temperature below the ambient temperature to form the retained austenite phase. Suppressing the carbide precipitation during bainitic transformation appears to be crucial for TRIP steels. Silicon and aluminum are also used to avoid carbide precipitation in the bainite region.

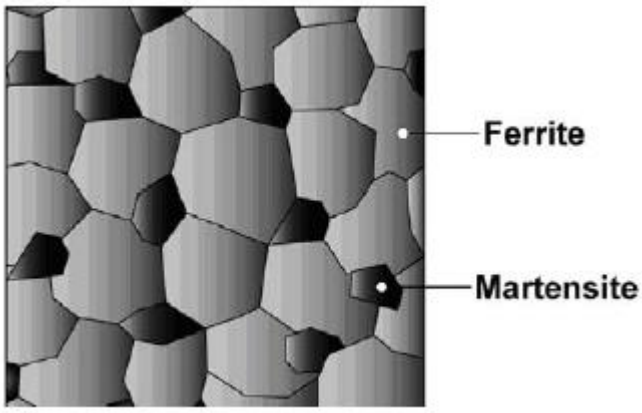

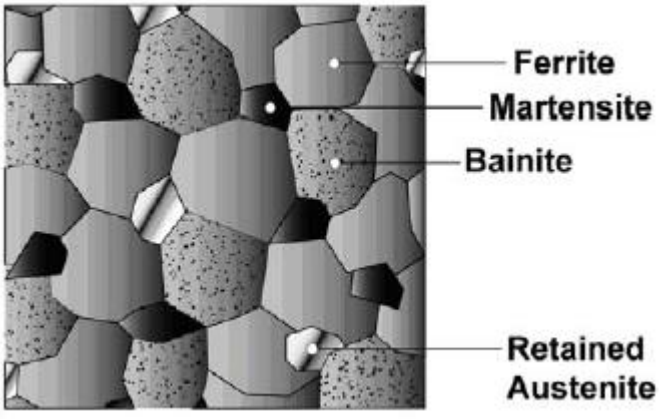

Fig.3.2 Schematic of DP microstructure **[22]**

Fig.3.3 Schematic of TRIP microstructure **[22]**

3.2.3 Complex Phase (CP) Steel

These steels are the transition to steel with very high ultimate tensile strengths (UTS). CP steels consist of a very fine microstructure of ferrite and a higher volume

fraction of hard constituent such as martensite, that are further strengthened by fine precipitates **(G. E. Opbroek 2009)**. CP steels uses many of the same alloying elements as found in DP and TRIP steels, but also often have small quantities of some other significant elements like niobium, titanium, and/or vanadium to form fine strengthening precipitates with the hard phases constituents. CP steels shows higher yield strengths for equal tensile strength levels of 800 MPa and greater. These steels are generally characterized by high formability, high energy absorption, and high residual deformation capacity.

3.2.4 Martensitic (Mart) Steel

In the formation of these steels, the austenite that exists during hot-rolling or annealing is transformed almost completely into the martensite during quenching on the run-out table or in the cooling section of the continuous annealing line. These steel can also be developed with post-forming heat treatment **(G. E. Opbroek 2009)**. These steels provide the highest strengths, ultimate tensile strength up to 1700 MPa. Martensitic steels are often subjected to post quench tempering to improve ductility or to reduce the hardenabillity, and can provide substantial formability even at extremely high strengths. Carbon is added to martensitic steels to increase hardenability and for strengthening the martensite.

3.2.5 Interstitial free (IF) steels

The term 'Interstitial Free' refers to the fact, that there are no interstitial solute atoms in the lattice of solid iron to strain, hence, resulting in a very soft steel which is known as 'Interstitial Free or IF steels' **(V. Gautam et. al 2017).** IF steels have matrix of interstitial free body centered cubic (bcc) ferrite. These steels normally have low yield strength, high plastic strain ratio, high strain rate sensitivity, good welding capacity and excellent formability.

Table 3.1: Chemical composition (in wt. %) of IF steel [2]

Element	C	Mn	Si	Al	Ni	Cr	S	P	Ti	Nb	Fe
Wt.%	0.004	0.112	0.002	0.043	0.002	0.012	0.009	0.017	0.026	0.018	Remaining

Chemical composition of IF steel is shown in table 1. Interstitial-free steels are ultra-low carbon steels and primary strengthening due to a combination of elements in solid solution with ferrite, precipitation of carbides and/or nitrides, and grain refinement with excellent formability. In this category of steel, titanium and niobium (or columbium) are added in very small percentage of volume to combine with the remaining residual amounts of carbon and nitrogen to make them interstitial free **(Wang and Wang, 2001)** and one common element added to increase strength is phosphorous (a solid solution strengthener). These sheets have been procured in two different thicknesses of 0.8mm and 1.5mm.

3.3 Properties of IF steel

- Ultra low stabilized carbon (C) and nitrogen (N) in sheet steel offer excellent mechanical properties, age hardening, and deterioration of the r-value (measure of resistance to thinning and drawability).
- IF steels made using only titanium (Ti) are very common and are used to achieve the best mechanical properties for deep drawing. It is very reactive in a zinc bath and is usually coated only as galvanized steel (GI).
- Another popular type of IF steel is that is stabilized with both titanium (Ti) and niobium (Nb). Depending on the relative amounts of Ti and Nb, this type of steel needs to be annealed at a higher temperature during galvanization and has slightly inferior mechanical properties to the Ti type. Ti-Nb type IF steel is also less reactive in a zinc bath and is usually employed when producing galvannealed steel (GA).
- IF steel made using addition of phosphorous (P) up to 0.06 %, combines excellent formability with higher strength, producing good dent resistance exterior panels.
- Most IF steels have manganese (Mn) levels below 0.20 %, and the formability increases as the carbon level is lowered.
- IF steels offer excellent drawability for their strength level as a result of their very good fracture elongation, normal strain ratios and strain hardening coefficients. These steels can be readily welded by all the welding processes.

3.4 Advantages of IF steel

- Superior stamping, forming, and drawing performance
- The ability to make more complex parts, perhaps using a fewer numbers of dies
- Age-hardening resistance (long shelf life for stored steel), and
- Improved coating adhesion for galvanized products.

The main limitation of IF steel is that it can be very soft, resulting in shearing and punching difficulties, and its use may result in parts that are not as 'strong', i.e., dent resistant, compared to parts made from carbon steel.

3.5 Application of IF steel

- With their high mechanical strength guaranteeing good fatigue and impact resistance, these steels are intended for structural parts (longitudinal beams, cross members, B-pillars, etc.) as well as for skin parts, in which they provide good indentation resistance.
- This steel type is widely used for both structural and closure applications, for manufacturing of complex automotive body parts such as dash panels, body side inners, fuel tanks etc. where high formability is required.
- The lack of interstitial atoms in the atomic structure enables IF steel to have extremely high ductility, ideal for deep-drawn products.
- In contrast to that of conventional drawing qualities, the weight reduction potential of these products increases with drawing depth.

3.6 Preparation of TWBs

Preparation of the TWBs from the steel sheets of different thickness was carried out in two steps:

1) Laser cutting of blanks and

2) Laser welding of blanks.

3.6.1 Laser cutting of blanks

To prepare the TWB's, blanks are prepared from two different sheets of IF steel with thicknesses of 0.8 mm and 1.5 mm. For cutting the blanks laser cutting is chosen due to its greater energy concentration, higher penetration rate and higher cutting speed. Lasers create narrow kerfs contrary to other available processes and thus achieve high-precision cuts. There is no sign of distortion shown by this method and even in many cases post-processing is not necessary as the component is subjected to only little heat input and it can mostly be cut dross-free.

Although blanking is a very fast and economical operation, the sheared edges generally undergo plastic deformation and the blanked sheets are rendered with bevel edges. These edges are not suitable for autogenous laser butt welding because the admissible gap and offset between the butting sheets should be of the order of 3-5% and 5-12% of sheet thickness of thinner sheet, respectively for a particular thickness combination **(Ready et al., 2001).** Therefore, in order to get a sound weld and ensure close fit up at the joint interfaces, preparation of proper butt edges with high degree of squareness and straightness were achieved by laser blanking of the procured sheets using a CO_2 laser of 4kW capacity (TRUMPF: Model-LC3030 with resonator: TLF4000 Turbo) at a cutting speed of 1.2 m/min.

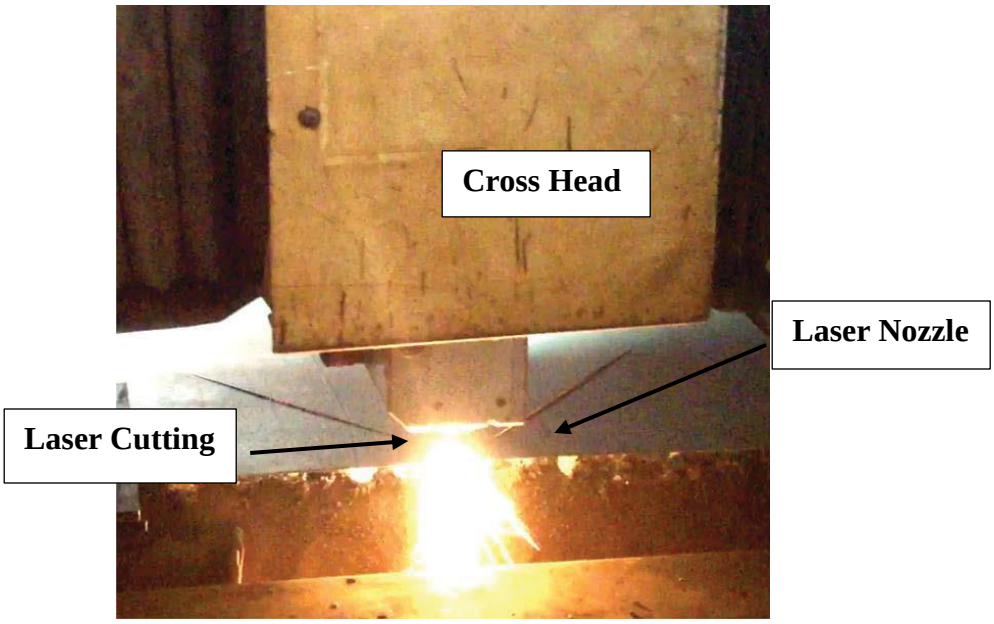

Fig.3.4: Laser blanking of sheets using CO_2 laser

During laser blanking, nitrogen gas was supplied under a high pressure of 6 bar so that the steel sheet was melted by the power of laser beam and blown out of the kerf by using the kinetic energy of the gas jet. Cutting with an inert gas (nitrogen gas) is often referred to as clean cutting or high pressure cutting. A laser power, which is the total amount of energy released in the form Cross head Laser cutting Laser nozzle of intense laser light of single wavelength per second, in the range of 1.4 to 1.5kW was employed for laser cutting the specimens of different steels and thicknesses. The intensity of the laser beam which is calculated by dividing the laser power by the area over which the power is concentrated. Therefore, focusing of a 1.5kW laser beam over a spot diameter of 0.2 mm resulted in a power density of approximately 190 kW per mm2.

3.6.2 Laser welding of blanks

Laser welding is one of the fusion welding process by irradiation of a concentrated laser beam. It is generally an autogenous welding technique which means no filler material is added during welding process and among the present various types of laser, Nd:YAG laser is preferred over other lasers for better absorption during welding of steels. In this study, TWBs of steel blanks of similar materials (IF steel) and dissimilar thicknesses (0.8mm and 1.5 mm) have been used due to their wide applications in various

sheet metal parts in the automobile industry. Precise control of gap between the blanks and misalignment to be welded are important parameters to obtain a good quality weld which may otherwise result in a poor weld and might adversely affect the formability of the TWBs.

The Nd:YAG laser system, a 4kW Oyabe Seiki (Model: TRUMPF TruDisk 4002 (Resonator)) was used for butt welding of different steel specimens. Technical specifications of the resonator TruDisk-4002, laser welding machine are given in Table 3.2.

Table 3.2: Technical specifications of resonator TruDisk 4002

Parameter	Value
Wavelength	1030 nm
Laser power	4000 W
Beam quality	8mm. mrad
Core diameter of fiber	200 μm

Although the principle of keyhole effect involved in laser cutting and welding is same, a high pressure inert gas is used in laser cutting to blow out the molten pool from the kerf, whereas inert gas is used in laser welding at low pressure to provide sufficient time for molten metal pool to solidify and joining of the butting surfaces of the metal.

The minimum size of the blanks was kept as 350mm X 350mm due to the size limitation of the fixtures of the laser system. These blanks were fed from both sides of the machine and were further taken to the welding place using a set of automated suction cups. Fig. 3.5 (a) shows the inside view of the welding bay with left and right side fixtures used for different blanks fed from sides in the machine for welding. Since the spot diameter of the beam when focused on the butting edges is about 0.2mm, position of the joint under laser must be precise enough so that beam spot does not miss the joint. It may otherwise result in the defective welds with problems of lack of fusion, sagged welds or

concave root surfaces. With the help of the machine controls and a dedicated computer as shown in Fig.3.5 (b), the movement of the sensor guided welding head was checked thoroughly using a sensor installed in front of laser focal point at the laser head. This procedure of checking is termed as 'seam teaching and tracking' of laser beam to analyze proper start and end of the weld as well as alignment of the part under the laser head.

Seam teaching has the advantage of being performed with the help of point to point movements which increases the accuracy and the synchronization errors can also be avoided. Argon was used as shielding gas to prevent the rapid oxidation of the weld pool and directed at a flow rate of 7 to 10 l/ min. Welds prepared in the presence of shielding gas are shiny and present more appealing look as well. A number of trials were carried out to achieve a sound free laser weld by varying the laser power and laser welding speed in the range of 2.7 kW to 3.4 kW and 6 to 7m/min, respectively.

(a) Fixtures in welding bay (b) Control panel

Fig.3.5: Inside view of Nd:YAG laser system of Make: Oyabe Seiki
(Courtesy: Caparo Mi Steel Processing Pvt. Ltd., Bawal, Haryana, India)

Argon as an inert shielding gas, protects the molten metal and HAZ from oxidation and increases the welding speed and thereby enhances mechanical properties of the joint. During laser welding with argon as shielding gas, a plasma cloud forms which is characterized by emission of bluish light but does not affect the penetration of the Nd:YAG laser beam due to its shorter wave length.

Laser power used to produce different thickness combinations of TWBs with successful welds are summarized in Table 3.2. A higher laser power was used in welding with increase in thickness ratio. Erichsen cupping test was conducted using a 20mm diameter hemispherical punch on TWBs of each thickness combination to quickly assess the formability and strength of the weld joint and each time the failure occurred on the thinner side of TWBs, clearly indicating that the weld joints are strong and sound.

3.7 Tensile properties of parent sheets

Tensile properties of the sheet metal greatly influence its deformation behavior in forming operations. The stress-strain curves are extremely important to define the material behavior in FE simulations because the data obtained from the stress-strain curves is entered to define the plastic properties of the material for the prediction of springback in V-bending. In order to determine the tensile properties of parent sheets in orientations that are parallel (0º), diagonal (45º) and perpendicular (90º) to the rolling direction, the tensile specimens were prepared as per ASTM-E8M full size specification (ASTM, 2008) with the help of CO2 laser cutting as shown in Fig.3.4.

All the specimens for tensile test were tested on a universal testing machine (UTM) of a 50 kN load capacity at a constant cross head speed of 2.5 mm/min as shown in figure 4.6 (b). From the load vs elongation data obtained from the UTM, engineering stress-engineering strain curves and true stress-true strain curves have been plotted.

Fig.3.6: (a) Laser cutting of full size tensile test specimens (b) Tensile testing using a 50kN UTM

To convert the data obtained from the load-elongation curve into the engineering stress-strain and into true stress-strain following equations have been used:

$$\sigma = \frac{P}{A_o}$$

$$\varepsilon = \frac{L_o - L_f}{L_o}$$

$$\sigma_t = \sigma\,(1+\varepsilon)$$

$$\varepsilon_t = \ln(1+\varepsilon)$$

Where P = load, A_o = original area, σ = engineering stress, ε = engineering strain L_o= original length, L_f= final length, σ_t= true stress and ε_t= true strain

As steel obeys general power law of strain hardening ($\sigma_t = K\varepsilon_t^n$), where σ_t and ε_t are true stress and true strain respectively, the values of strain hardening exponent (n) and strength co-efficient (K) have been determined from $ln\sigma_t$ - $ln\varepsilon_t$ plots considering the data from within the uniform plastic deformation range.

The normal anisotropy or the average plastic strain ratio ($\bar{R}$) of the parent steel sheets has also been determined from the uni-axial tension test of specimens oriented at

$0^o, 45^o \; and \; 90^o,$ with respect to the rolling direction as per ASTM E517-06. In order to evaluate *R* (plastic strain ratio) value, tensile specimens were plastically deformed to 20% elongation and cross head was stopped in automatic mode with the options available in a dedicated software Tenius Olsen Horizon supplied with the machine. The width and the gauge length before and after the test were measured with a digital vernier caliper and plastic strain ratio was calculated in all the three directions w.r.t the RD using following equations:

$$R = \frac{\varepsilon_w}{\varepsilon_t} = \frac{\varepsilon_w}{-(\varepsilon_t + \varepsilon_l)} = \left[\frac{\ln\left(\frac{\varepsilon_f}{\varepsilon_o}\right)}{\ln\left(\frac{l_o \cdot \varepsilon_o}{l_f \cdot \varepsilon_f}\right)}\right]$$

Where w_o and l_o are initial width and length, w_f and l_f are final width and length, ε_w is true width strain, ε_t is true thickness strain and ε_l is true longitudinal strain.

The values of plastic strain ratio determined in three different directions as mentioned above were used to determine normal anisotropy ($\bar{R}$) , using the standard formula as given below:

$$\bar{R} = \left(\frac{R_o + 2R_{45} + R_{90}}{4}\right)$$

Where the notations R_o, R_{45} and R_{90} indicate the plastic strain ratio of the specimens oriented at 0°, 45° and 90° with respect to the rolling direction. $\bar{R}$ value is very sensitive to errors, especially in width measurement and depends upon the accuracy of flatness and squareness of the edges prepared. Therefore, all the tensile specimens were prepared by laser cutting for accurate determination of plastic strain ratio.

3.8 Tensile properties of TWBs

Tensile properties of TWB's are equally significant as parent sheet metal to determine the behaviour of TWB's during forming operations. For tensile testing of TWBs, subsize tensile specimens (as per ASTM-E8M standard) of TWBs of different thickness combination (0.8 mm and 1.5 mm) were prepared using the Wire-cut Electrical Discharge Machining (WEDM) technique. The tensile specimens of TWBs with weld

orientation at 0°, 45° and 90° w.r.t. rolling direction (RD) are shown schematically in figure_. To prepare a sub-sized tensile specimen of gauge width 6.25mm, a reference hole at the middle of the weld zone of small diameter was drilled using a wire cut-electric discharge machine. This reference hole helped to locate the weld region in the middle and parallel to the tensile axis of the specimens. During preparation of the specimens, the weld line orientation was kept at 0º (parallel), 45º (inclined) and 90º (transverse) w.r.t. the RD. These specimens were also tested on the 50 kN UTM at a speed of 2.5mm/min for determination of tensile properties of welded specimens at different orientation w.r.t. RD.

3.9 Experimental procedure for V-bending and spring-back measurement

To determine the springback behaviour of TWBs, a series of bending tests were conducted on TWBs of IF steel of thickness combination 0.8 mm and 1.5 mm, were used in the bending experiments carried out on a UTM machine using a V-bend die-punch set with three different punch profile radius of 10 mm, 12.5 mm and 15 mm.

An experimental set up has been developed for determination of springback in V bending which is responsible for the generation of residual stresses in TWB's. For conducting bending experiments of TWBs three sets of V- bend die and punch with an included angle of 90° with three different punch radius has been used. The punches were designed to have profile radius of 10 mm, 12.5 mm and 15 mm and dies with corresponding profile radius and clearances as shown in Fig._. The clearance was kept equal to the sheet thickness in order to prevent any localized compression at the bottom of the die. The dies and punches were machined from AISI D2 steel by using WEDM process. AISI D2 steel is a tool steel containing 1.6% carbon, 12% chromium, 1.0% molybdenum and 1.0% vanadium. This steel is preferred for cold working dies and tools due to high wear resistance and compressive strength.

V-bending experiments were carried out on the UTM machine with load capacity of 50 kN. The punch shank was secured in the grip mounted on the movable cross head, and the die was fixed to the stationary wedge grip as shown in Figure (b).

The bend specimens were cut by WEDM process, with dimensions 150mm × 25mm to ensure plane strain condition for which the width should be at least 10–15 times the sheet

thickness. It was ensured that the weld line was exactly at the center of the width in case of specimens of TWBs for V-bending. During bending tests, the flat surface of TWB specimen was kept towards the punch side, and a filler sheet, whose thickness was equal to the thickness difference in TWBs, was used between the die and the blank to prevent any twisting. However, depending upon the thickness ratio, small twisting is expected in normal bending operations. Higher the thickness ratio, higher may be the twisting due to higher magnitude of unbalanced force, if the shims are not used. A punch speed of 20 mm/min was adopted in all the experiments. The displacement of the punch was kept equal to the die depth during bending experiments and it was controlled precisely by a dedicated software. A vision inspection system with a probe sensor was used to measure the final included angle in the tested bend specimens. Each tested specimen was secured in a magnetic V-block and measured twice for interior included angle using a probe by touching at four points on each arm of the tested specimens. The initial included angle (θ_o) was measured on the die.

3.9.1 Modelling and Simulations

In this study, all the simulations were performed using ABAQUS software in two steps – loading and unloading. For the V bending simulations (the loading step) ABAQUS–Explicit solution procedure was adopted as it can handle nonlinear complicated contact problems with ease in a shorter time **(V. Gautam et. al 2017)**. The completed bending simulation model was exported from ABAQUS-Explicit to ABAQUS–Implicit to conduct springback simulations (the unloading step). Springback simulations offered lower nonlinearity as the unloading was done by removing the punch and die constraints from the model.

In order to understand the plastic deformation during bending and its effect on springback phenomenon, simulations for bending were carried out for TWB 0.8mm and 1.5mm thickness combination. The bending simulations were carried out for TWB during which the specimens for bending with dimensions 150mm×25mm were modelled (Figure 3.7) as deformable surfaces defining the top surface of the blank as a homogeneous continuum shell, and the thickness of the TWB was assigned as thickness 0.8mm for thinner sheet, 1.8mm for thicker sheet and 1.15mm for the weld zone.

The thickness integration by the Simpson rule with 5-point integration (a default value in ABAQUS) was adopted for TWB specimens. Prediction of springback depends upon the integration scheme and integration points through sheet thickness. Many researchers have shown in their studies that 5 to 7 integration points are optimal and more than that will not affect the accuracy of springback prediction. Since the amount of springback depends on bending moment which in turn depends on stress distribution in sheet thickness, shell elements require numerical integration of stress and strain through thickness to determine bending moment and the force. The number of integration points directly affects the simulation time, and therefore, the Simpson rule with 5 integration point's method was adopted.

The specimens of TWB for bending simulations were modelled containing three different regions, that is, two parent materials with different thickness combination and a weld zone as shown in Figure 3.7. The top surface of the TWB was first modelled and then the respective thicknesses were assigned to the regions of the two parent materials. The shell thickness in the weld zone was taken to be average of the thicker and the thinner sheets. The mesh size in the weld zone was kept finer for better results. The mesh size was arrived on the basis of the maximum Von Mises stress in the deformed region, that is, the mesh was refined until the stress in the specific region does not change significantly (\1.8%). However, if the mesh is too dense, it requires a large amount of computer memory and long run time to perform the simulation.

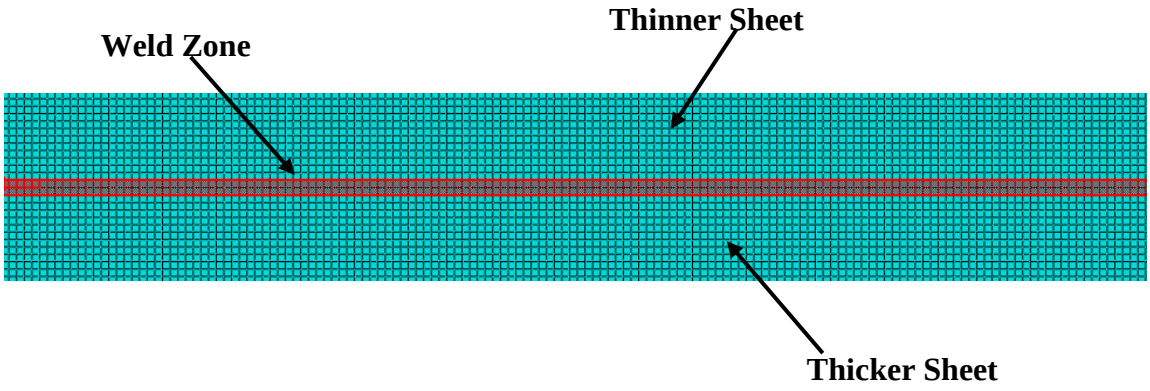

Fig.3.7: A TWB meshed with shell elements.

The punch and die were modelled as analytical rigid shell, whereas the blank as deformable shell planar with S4R shell elements. The S4R shell element is a four node thin shell element with reduced integration, hourglass control and finite member strains. To compute the dynamic response of analytical rigid die and punch, a point mass of 10 kg was assigned to the reference point on both of these rigid bodies. In order to enhance accuracy and efficiency, quasi-static analysis demands that the application of bending load be as smooth as possible. Sudden jerky load application creates stress waves in the blank inducing noisy and inaccurate solution. Load application in a gradual manner requires that the acceleration changes by only a small amount from one increment to the other. This results in the gradual change in velocity and displacement. The explicit method has an inbuilt amplitude curve that creates smooth loading amplitude which was assigned to the reference point on the punch. A typical bending simulation is shown in Figure 3.8.

For the springback simulations, the procedure adopted was static-general (ABAQUS standard) with non-linear geometry. This method utilizes Newton–Raphson method to determine the solution for nonlinear problems. This method breaks the simulation into a number of load increments and finds the approximate equilibrium configuration at the end of each load increment. As a result of this, several iterations were made to determine an acceptable solution to a given load increment. After removing all the die and punch constraints in the model, the blank was assigned initial state of previous bent data file containing history of loading. A central node in the blank was assigned a zero velocity so that the results are contained about the same node. For springback measurement, node coordinates were captured for loaded and unloaded frames. The coordinate points for both the frames were plotted in CAE interface and the difference between the two gives the springback. The change in bend angle due to springback as obtained in simulations as shown in figure_.

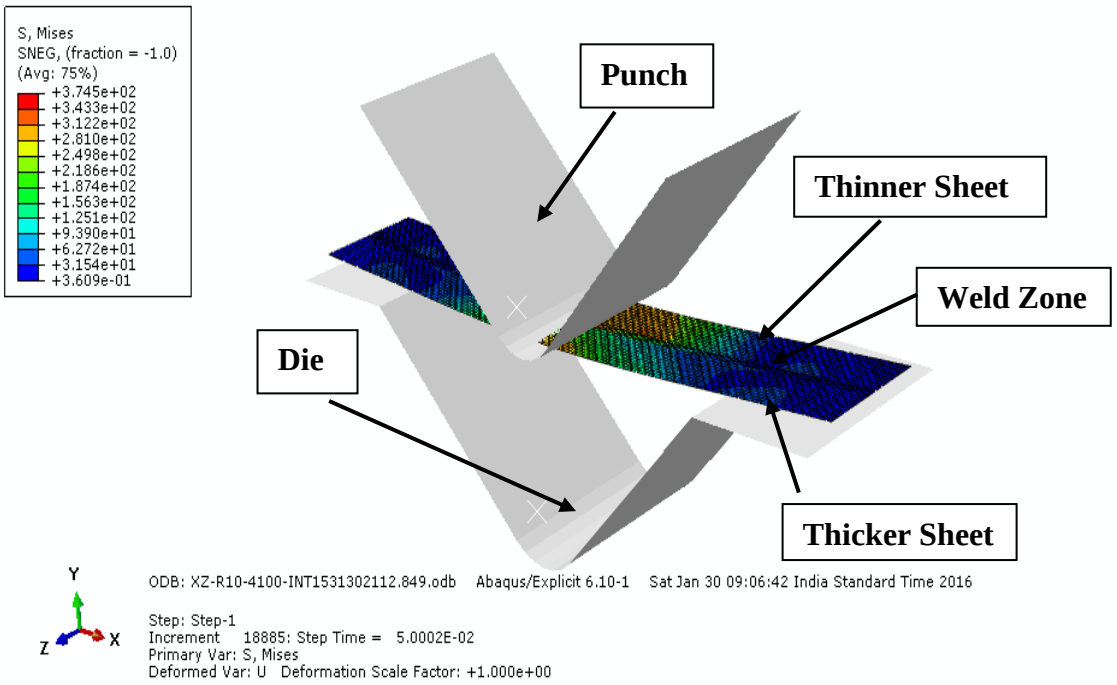

Fig. 3.8: Simulation of V-bending of TWB.

3.10 Experimental procedure for measurement of residual stress

Presence of weld zone which is responsible for the generation of residual stresses in TWB, significantly affect the behavior of TWB during forming processes. Hence to eliminate the possibility of failure caused by the presence of residual stresses, their variation and characterization within the TWB is necessary.

As discussed earlier there are both destructive and non-destructive methods are available for the experimental measurement of residual stress. In this study, Pulstec μ360 X-ray residual stress analyzer is used for the experimental investigation of residual stresses in TWBs of IF steel due to springback after bending with three different punch profile radius of 10mm, 12.5mm and 15mm.

X-ray diffraction uses two different methods $\sin^2\Psi$ and $\cos\alpha$ for the measurement of residual stress which are explained below.

3.10.1 Fundamental concepts in X-ray diffraction

Basically, diffraction methods involve in determination of residual stress, measure the angles at which the incident x-ray diffracted with maximum intensity when a crystalline sample is subjected to X-rays. From this maximum angle it is possible to obtain the interplanar spacing (d) of the diffraction planes using Bragg's law. If the residual stresses exist within the sample, then the internal spacing (d) will be different than that of an unstressed state (d_o). This difference is used to calculate the strain value, which is proportional to magnitude of the residual stress.

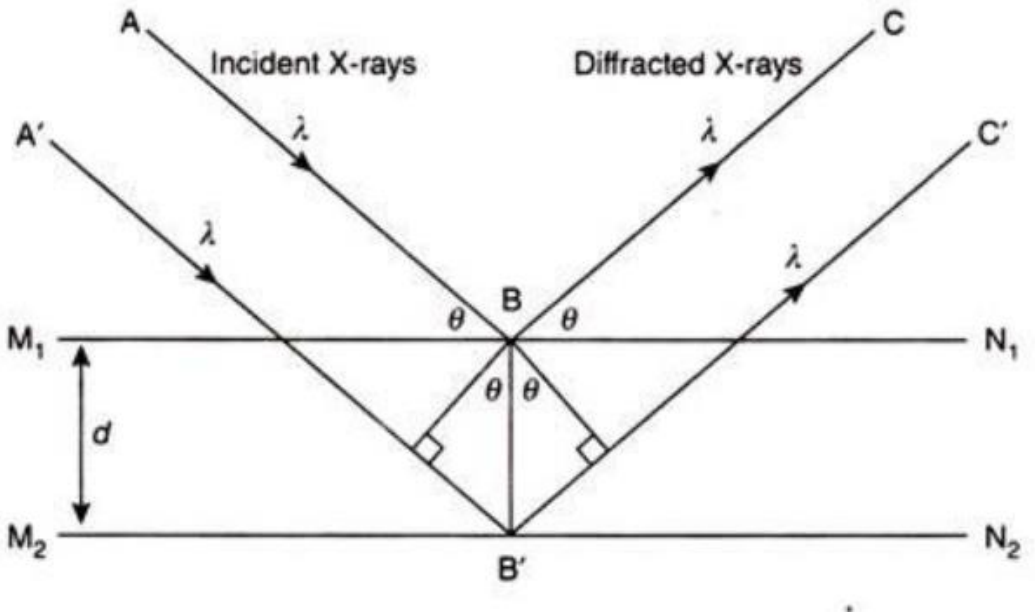

Fig. 3.9: Principle of X-ray diffraction analysis **[22]**

The fundamental law which govern the phenomenon of diffraction of incident X-ray beam is Bragg's law which states that, "for a crystalline solid, the waves are scattered from lattice planes separated by the interplanar distance d. When the scattered waves diffracted constructively, they remain in phase with each other but the path difference between the two waves is equal to an integer multiple of the wavelength. The path difference between two waves undergoing interference is given by $2d\sin\theta$, i.e.

$$n\lambda = 2d \sin\theta$$

Where n is a positive integer, λ is the wavelength of the incident wave and θ is the scattering angle.

3.11 Calculation of stresses by X-ray diffraction

In this section the fundamental concepts related to X-ray diffraction which was discussed in the previous sections will be combined in the derivation of the equations of the residual stress measurement. It is very important to note that by x-ray diffraction stress is not measured directly; in actual it is always strain value that is obtained by measuring the difference between the inter-planar spacing d for free and stressed state and then the value of stress is measured by using appropriate equations of elasticity.

X-ray diffraction method uses two different techniques $\sin^2\Psi$ and cosα for the measurement of stress which are explained below.

3.11.1 $\mathbf{Sin^2\Psi}$ method-

$Sin^2\Psi$ technique using X-ray diffraction method of residual stress determination basically measure the angles (Ψ) at which the maximum diffracted intensity take place when a crystalline sample is subjected to x-rays **(O. Anderoglu 2004).** From these angles it is possible to obtain the interplanar spacing (d) of the diffraction planes using Bragg's law. If the residual stresses exist within the sample, then the d spacing will be different than that of an unstressed state (d_o). This difference is proportional to the strain value and then magnitude of the residual stress is calculated.

The diffractometer is the most common apparatus used for determining diffraction patterns for each value of Ψ i.e. 0^o, 30^o, 60^o, 90^o……..etc. By obtaining the diffraction pattern from diffractometer for each value of Ψ a graph peak (intensity) vs 2θ can be drawn. With the help of the graph we can easily identifies the value of 2θ for which peak or intensity is maximum and then putting that value of θ in the Bragg's law equation we can get the value of inter-planar spacing d for the incident beam of known wavelength (λ). Hence, the strain by measuring the difference between the d and d_o is calculated and corresponding value of stress is obtained by using proper elastic constants.

As shown in figure 3.10 an orthogonal coordinate systems which is used to derive equations. The axes S_i are for the surface of the sample with S_1 and S_2 on the surface. L_i define the laboratory system with L_3 is in the direction of the normal to the planes (hkl) whose interplanar spacing d will be measured. L_2 makes an angle φ with S_2 and is in the plane which is defined by S_1 and S_2. When the inter-planar lattice spacing d is obtained from the diffraction peak for a given reflection hkl, the strain component along L_3 can be obtained using the formula

$$\varepsilon'_{\phi\psi} = \frac{d_{\phi\psi} - d_o}{d_o}$$

Where $d_{\phi\psi}$ and d_o are stresses and unstressed interplanar spacing and $\varepsilon'_{\phi\psi}$ is the strain in L_3 direction.

(Primed components refer to laboratory system L_i whereas unprimed components refer to the sample coordinate system, S_i)

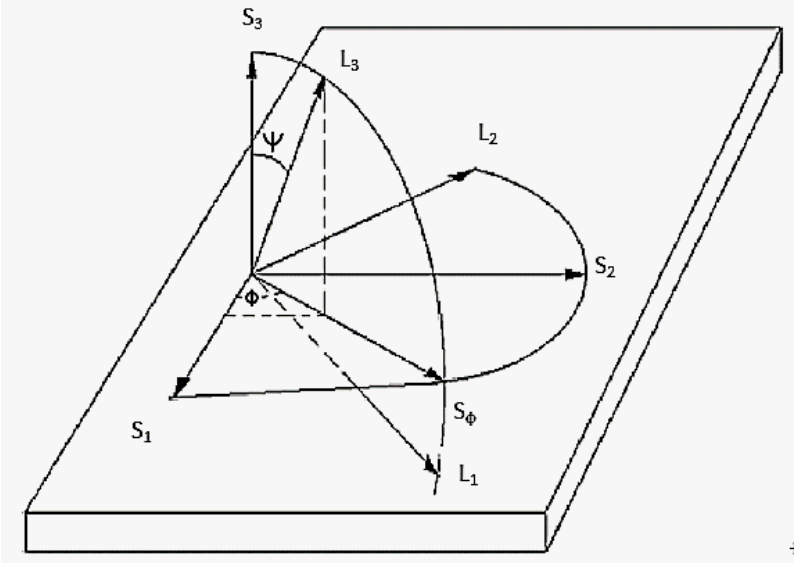

Fig.3.10: Sample and laboratory coordinate systems

Here S_i = Sample coordinate system

L_i = Laboratory coordinate system

Now we transform this strain component into the sample system by using the rotation matrix of tensor transformation

$$(\varepsilon'_{ij})_{\phi\psi} = a_{ik}\, a_{jl}\, \varepsilon_{kl}$$

$$(\varepsilon'_{33})_{\phi\psi} = a_{3k}\, a_{3l}\, \varepsilon_{kl} \ldots\ldots \quad (1)$$

Where a_{3k} = direction cosine between L_3 & S_k

a_{3l} = direction cosine between L_3 & S_l

Direction cosine matrix for tensor transformation

$$a_{ik} = \begin{vmatrix} a_{11} & a_{12} & a_{13} \\ a_{21} & a_{22} & a_{23} \\ a_{31} & a_{32} & a_{33} \end{vmatrix} = \begin{vmatrix} \cos\phi\cos\psi & \sin\phi\cos\psi & -\sin\psi \\ -\sin\phi & \cos\phi & 0 \\ \cos\phi\sin\psi & \sin\phi\sin\psi & \cos\psi \end{vmatrix}$$

Substitute a_{3k} , a_{3l} in equation (1)

$$(\varepsilon'_{33})_{\phi\psi} = \frac{d_{\phi\psi} - d_o}{d_o} = a_{31}a_{31}\varepsilon_{11} + a_{31}a_{32}\varepsilon_{12} + a_{31}a_{33}\varepsilon_{13} + a_{32}a_{32}\varepsilon_{22} + a_{32}a_{33}\varepsilon_{23} + a_{33}a_{33}\varepsilon_{33}$$

To calculate stress (or strain) tensor at sampling gauge location at least 6 independent measurement of strains in different direction of $\varepsilon\,\{\phi,\psi\}$

So

$$(\varepsilon'_{33})_{\phi\psi} = \cos^2\phi\sin^2\psi\,\varepsilon_{11} + \sin 2\phi\,\sin^2\psi\,\varepsilon_{12} + \cos\phi\sin 2\psi\,\varepsilon_{13} + \sin^2\phi\sin^2\psi\,\varepsilon_{22} + \sin\phi\,\sin 2\psi\,\varepsilon_{23} + \cos^2\psi\,\varepsilon_{33} \ldots\ldots \quad (2)$$

Equation (2) is the basic equation that is used in x-ray diffraction strain measurement.

3.11.2 For linear $d_{\phi\psi}$ vs $\sin^2\psi$ behavior (No Ψ splitting i.e. $\varepsilon_{13} = \varepsilon_{23} = 0$)–:

$$\varepsilon_{ij} = \begin{vmatrix} \varepsilon_{11} & \varepsilon_{12} & 0 \\ 0 & \varepsilon_{22} & 0 \\ 0 & 0 & \varepsilon_{33} \end{vmatrix}$$

So equation (2) becomes

$$(\varepsilon'_{33})_{\phi\psi} = \cos^2\phi\sin^2\psi\,\varepsilon_{11} + \sin 2\phi\,\sin^2\psi\,\varepsilon_{12} + \sin^2\phi\sin^2\psi\,\varepsilon_{22} + \cos^2\psi\,\varepsilon_{33}$$

$$(\varepsilon'_{33})_{\phi\psi} = \{\varepsilon_{11}\cos^2\phi + \varepsilon_{12}\sin 2\phi + \varepsilon_{22}\sin^2\phi\}\,\sin^2\psi + \cos^2\psi\,\varepsilon_{33}$$

$$(\varepsilon'_{33})_{\phi\psi} = \{\varepsilon_{11}\cos^2\phi + \varepsilon_{12}\sin 2\phi + \varepsilon_{22}\sin^2\phi - \varepsilon_{33}\}\,\sin^2\psi + \varepsilon_{33}$$

3.12 Calculation of stress

Stress values of sample coordinate system can be calculated using general form of hook's law

$$\sigma_{ij} = c_{ijkl}\,\varepsilon_{kl} \quad \text{..... (3)}$$

Where c_{ijkl}= Stiffness tensor quantity of fourth order

Stresses in any other coordinate system can be determined using tensor transformation

$$\sigma'_{ij} = a_{ki}a_{kl}\sigma_{kl}$$
$$= a_{1i}a_{1j}\sigma_{11} + a_{1i}a_{2j}\sigma_{12} + a_{1i}a_{3j}\sigma_{13} + a_{2i}a_{1j}\sigma_{21} + a_{2i}a_{2j}\sigma_{22}$$
$$+ a_{2i}a_{3j}\sigma_{23} + a_{3i}a_{1j}\sigma_{31} + a_{3i}a_{2j}\sigma_{32} + a_{3i}a_{3j}\sigma_{33}$$

Reverse of equation (3)

$$\varepsilon_{ij} = \delta_{ijkl}\sigma_{kl} \quad \text{..... (4)}$$

Where δ_{ijkl}= Elastic tensor

When equation (4) is substituted in equation (2), the relation between the stresses & measured data is obtained.

General equation for an isotropic & homogeneous material to link measured d values to the stresses in the sample coordinate system

$$\varepsilon_{ij} = \frac{1+\upsilon}{E}\sigma_{ij} - \delta_{ij}\frac{\upsilon}{E}\sigma_{kk} \quad \text{..... (5)}$$

Here $\delta_{ij} = 1\ if\ i \neq j$

$\delta_{ij} = 0\ if\ i = j$

Substitute the equation (5) in (2)

So

$$\varepsilon = \frac{d\Phi\Psi - do}{d_o}$$

$$= \frac{1+\upsilon}{E}\{\sigma_{11}\cos^2\phi + \sigma_{12}\sin 2\phi + \sigma_{22}\sin^2\phi - \sigma_{33}\}\sin^2\psi + \frac{1+\upsilon}{E}\sigma_{33}$$
$$-\frac{\upsilon}{E}tr(\sigma) + \frac{1+\upsilon}{E}\{\sigma_{13}\cos\phi + \sigma_{23}\sin\phi\}\sin 2\psi$$

For Bi-axial stresses

$$\varepsilon = \frac{d\phi\Psi - do}{d_o} = \frac{1+\upsilon}{E}\{\sigma_{11}\cos^2\phi + \sigma_{12}\sin 2\phi + \sigma_{22}\sin^2\phi\}\sin^2\psi - \frac{\upsilon}{E}(\sigma_{11}+\sigma_{22})$$

$$\boxed{\varepsilon = \frac{d\phi\Psi - do}{d_o} = \frac{1+\upsilon}{E}\sigma_\phi \sin^2\psi - \frac{\upsilon}{E}(\sigma_{11}+\sigma_{22})}$$

Where σ_ϕ is the stress component along S_ϕ direction. It is given by

$$\sigma_\phi = \sigma_{11}\cos^2\phi + \sigma_{22}\sin^2\phi$$

3.13 Cosα method

The standard $\sin^2\Psi$ approach with a point detector (diffractometer) requires a series of measurements at different orientations of the sample with respect to diffractometer to obtain the projection of the strain tensor along the several different orientations of the scattering vector, and these orientations are chosen so as to simplify the subsequent analysis **(N. Peterson et. al).**

Since for a defined sample orientation in laboratory coordinates every point in the Debye ring comes from a different orientation of the scattering vector, when using a 2D detector the whole

Debye ring can be used and a set of scattering vector orientations are simultaneously probed in a single measurement. Among the analysis methods that can be used to extract the stress state from such information with a single measurement, the "cosα" method was first proposed by Taira **(Taira et al, 1978)**.

Nowadays, use of portable residuals stress analyzers have seen increased due to the ease of its use. The cosα method has emerge as a faster and easier method of measuring residual stresses experimentally by using portable devices due to its ability to measure an entire Debye ring at once from the two dimensional detector, thus not requiring multiple sample tilts as in case of $\sin^2\Psi$ method **(Kobayashi et al. 2017).**

3.13.1 Portable X-Ray Device to Measure Residual Stress by using Cosα method

A portable X-ray device (μ-X360 residual stress analyzer from Pulstec Industrial Co.Ltd.) mounted on a robust table, is used to measure the residual stresses after springback in TWBs specimens **(Ling & Lee 2015).** Various points are marked across the width of the specimen after bending along the bend axis on thicker and thinner sheets both on compression and tension side. Detector gun of the stress analyzer is inclined at an angle of 35° for the IF Steel (Ferrite) to get the accurate results as shown in the figure 3.11(a).

Specimen is placed on the adjustable table exposing the surface to be assessed for the residual stress establishing a red spot of laser (approximately 2mm) on the mark where the X-ray beam will incident. The setting of the specimen is achieved by focusing a green check box which shows the specified area under inspection by sensors as shown in the figure 3.11(b).

A dedicated μ360 Residual Stress Measurement System Software Version 2.5.6.0 is used to make the measurements. Value of the residual stress with certain deviation is obtained from the data acquisition system. Similar procedure is repeated for all the points marked on the specimen both on compression and tension side of the specimens. The specifications of the instrument is given in Table 3.3.

(a) (b)

Fig.3.11: (a) Experimental set-up for residual stress measurement using portable X-ray machine (μ-X360) and (b) focus of collimator on bent specimen using laser.

Table 3.3: Specifications of the X-ray machine (μ-X360)

X-ray Tube Voltage, Current	30 KV, 1.0 mA
Target Material	Chromium (Cr)
Beam Wavelength (Energy)	λ= 2.29 Å (E = 5.4 KeV)
Collimator and Beam Spot Size	1 mm and 2 mm diameter
Sample to Detector Distance Approx.	35-40 mm
Typical Data Acquisition + Readout Time	90 seconds

3.14 Calculation of residual stress by the Cosα method

This method acquire the full Debye-Sherrer ring. A Debye-Scherre ring is obtained by using an image plate (IP) and the data obtained from image as analyzed for determining the value of stress. The translation of the laboratory system (diffractometer system) to the sample system is inherently more complex due to the 2D planar geometry of the measurement.

Where

θ = Angle of X-ray diffraction.

α = Azimuth angle of Debye-Sherrer ring.

η = Angle b/w incident beam and plane of strain measurement.

Ψ = Angle b/w plane normal to the specimen and plane of strain measurement.

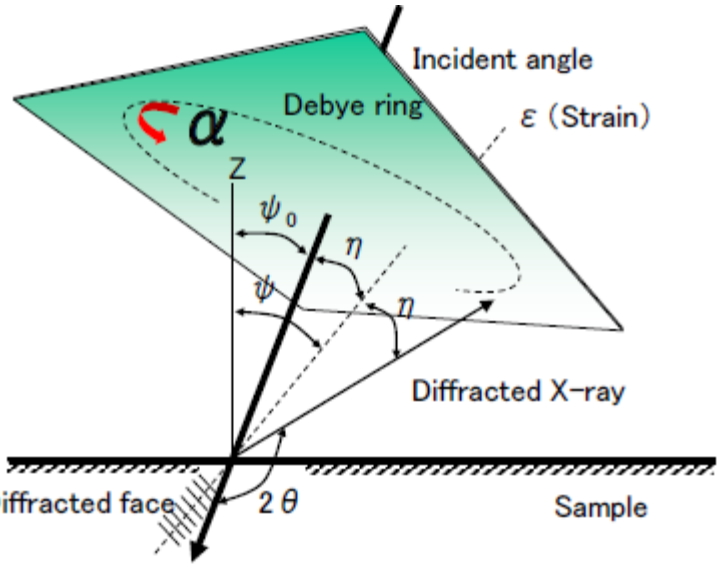

Fig.3.12: Geometric representation of the angles α, Ψ, η and 2θ on the Debye ring. **[24]**

The expression for the translation of strain,

$\varepsilon_\alpha = n_i n_j \varepsilon_{ij}$

Where n is the diffraction vector, which can be expressed in the form

$$n = \begin{bmatrix} \cos\eta \sin\psi_o + \sin\eta \cos\psi_o \cos\alpha \\ \cos\eta \sin\psi_o sin\emptyset_o + \sin\eta \cos\psi_o \sin\psi_o \cos\alpha + sin\eta cos\emptyset_o \, sin\alpha \\ \cos\eta \cos\psi_o - \sin\eta \sin\psi_o \cos\alpha \end{bmatrix}$$

Now this value of n can be inserted into Hooke's law to form

$$\varepsilon_\alpha = \frac{1+\upsilon}{E} n_i n_j \varepsilon_{ij} - \frac{\upsilon}{E}\sigma_{kk}$$

The magnitude of strain is determined from the detected position of the Debye-Scherrer ring. Calculate using the following formula.

$$\varepsilon_{\alpha 1} = \frac{1}{2}\{(\varepsilon_\alpha - \varepsilon_{\pi+\alpha}) + (\varepsilon_{-\alpha} - \varepsilon_{\pi-\alpha})\}$$

$$\varepsilon_{\alpha 2} = \frac{1}{2}\{(\varepsilon_\alpha - \varepsilon_{\pi+\alpha}) - (\varepsilon_{-\alpha} - \varepsilon_{\pi-\alpha})\}$$

Hence the value of stress is calculated from the strain using proper elastic and other constants.

$$\boxed{\sigma_x = -\frac{E}{1+\upsilon} \cdot \frac{1}{\sin 2\eta} \cdot \frac{1}{\sin 2\psi_o} \cdot \left(\frac{\partial \varepsilon\alpha_1}{\partial \cos\alpha}\right)}$$

CHAPTER 4

RESULTS

4.1 Tensile Properties of Parent Sheets and TWBs

The tensile properties of the IF steels of different thicknesses and in different orientations with respect to the rolling direction are given in Table 4.1. Elastic modulus of the steel is lower in thinner sheet than the thicker sheet and varies from 196GPa to 199GPa, whereas in thicker sheet it varies from 200GPa to 205GPa. The yield strength and ultimate tensile strength of the specimens oriented at 45° to the rolling direction are higher than the other orientations in both the thicknesses. The average percentage elongation of the thicker sheet is higher than the thinner sheet and is approximately 43%. In case of both the thicknesses, the average strain hardening exponent is approximately 0.33, which indicates excellent stretchability with uniform deformation. The average plastic strain ratio of the thicker sheet is lower than the thinner sheet which indicates the better drawability with thinner sheet.

Table 4.1: Tensile properties of Interstitial Free steel

Sheet thickness (mm)	Orientation w.r.t. RD	Elastic Modulus E (GPa)	Yield Stress (MPa)	Ultimate Tensile Strength (MPa)	% Elongation	Strain hardening exponent n	Strength coefficient K (MPa)	Plastic strain ratio R	Normal anisotropy $\bar{R}$
0.8	0°	196 ±1.0	108 ±0.5	249 ±1.7	42.9 ±1.42	0.32 ±0.006	526 ±11.9	1.99 ±0.07	1.92
	45°	196 ±5.2	118 ±1.0	254 ±2.0	43.7 ±0.25	0.30 ±0.005	522 ±5.2	1.69 ±0.06	
	90°	199 ±0.7	110 ±1.0	240 ±6.9	42.1 ±2.55	0.33 ±0.002	517 ±3.1	2.18 ±0.07	
1.5	0°	204 ±3.2	107 ±2.5	271 ±1.5	44.8 ±1.85	0.33 ±0.017	547 ±0.5	2.02 ±0.05	1.79
	45°	200 ±2.6	109 ±5.5	270 ±3.0	43.1 ±1.62	0.33 ±0.006	547 ±1.5	1.59 ±0.06	
	90°	205 ±1.3	109 ±3.3	265 ±1.5	43.9 ±1.38	0.33 ±0.015	550 ±10.7	1.91 ±0.08	

The results of tensile tests performed on specimens of longitudinally welded TWBs are summarized in Table 4.2. It is observed that yield strength and tensile strength of TWBs are much higher than the parent sheets but the average elongation is limited to 38% only indicating reduced ductility. The value of strain hardening exponent of the TWB specimens have also been reduced to 0.27 on an average basis. The higher values of tensile strength and lower values of strain hardening exponent and elongation can be attributed to the weld zone. The weld zone influences the overall mechanical properties of TWB.

Table 4.2: Tensile properties of TWBs of IF steel

Thickness combination (mm x mm)	Weld orientation w.r.t. RD	Yield Stress (MPa)	Ultimate Tensile Strength (MPa)	% Elongation	Strain hardening exponent *N*	Strength coefficient (MPa) *K*
1.5X0.8	0°	151±8.00	256±6.5	36.7±4.45	0.27±0.02	484±2.91
	45°	152±7.40	278±2.8	34.9±5.86	0.28±0.02	522±1.20
	90°	155±2.80	258±1.4	43.7±4.94	0.26±0.01	484±1.31

4.2 Simulation

In this study, ABAQUS software is used for the simulation of tailor welded blanks made of IF steel with thickness combination of 0.8 and 1.5 mm for the punch profile radius of 10 mm, 12.5 mm and 15 mm both loading (bending) and unloading (springback) condition. The punch and the die are modelled as analytical rigid whereas the blank is modelled as deformable one. Shell planar elements (S4R) are selected for the blank which is placed on the flat surface of the die. An inertia of 10 kg is assigned to the analytical rigid bodies i.e. die and punch. Surface to surface explicit (general) contact properties having tangential behavior are used for the interaction between punch and blank surface, between die and blank surface. Tangential behavior having penalty contact method is preferred for pinched contact of shells and rigid bodies. The coefficient of friction is assigned as 0.125 between blank-die and 0.05 between blank-punch surfaces. The die is made fixed and the punch is allowed to move equal to the die depth by assigning displacement/encastre boundary condition to the punch. Hill's anisotropic yield criterion, is used as a material model for deformable blank. The true stress-true strain data obtained from uniaxial tension test is used in the material model for TWBs. Although, studies are restricted to the determination of longitudinal stress after bending and springback, the weld zone is not modelled in the TWBs. A 5-point integration method using Simpson Rule is adopted to determine the longitudinal stress variation through the thickness of the blank.

In order to determine the residual stress after springback, the simulations are performed by removing the punch and the die from the FEA model. The blank is assigned initial history data of the bending simulation containing history of loading. A central node is assigned with zero velocity boundary condition so that the blank does not move from its initial position but both the arms of the blank are free to move in response to the removal of the constraint. The co-ordinates of the blank before and after springback are captured and the springback is determined as the difference in the bend angle before and after springback. The longitudinal stress variation located in the deformed zone across the width of the specimen and along the bend axis are also captured.

4.3 Variation of Longitudinal stress with punch profile radius

Variation of longitudinal residual stress with three different punch profile radius on springback in TWBs has been analyzed by using the data of longitudinal stress before and after springback at different points of integration through thickness. These variations across the width obtained from simulations of TWBs of IF steel for the thickness combination of 0.8mm and 1.5mm with different punch profile radius of 10 mm, 12.5 mm and 15mm. It is observed that the outer surfaces of the specimen show tensile stresses and inner surfaces show compressive stresses across the width for all punch profile radii. On unloading the specimen, residual stresses are generated as a result of springback. The outer surface has compressive stress and inner surface tensile.

As shown in figures 4.1(a), 4.2(a) and 4.3(a), before springback the stress values at the outermost integration points are almost constant in the center but lower at edges, whereas a sudden increase in the value is observed at the junction of thicker sheet and the weld zone, then the stresses in weld zone first decreases slightly and then increases by a very small value. Although, the variation of stresses in weld zone is almost constant. Now there is a sudden decrease in the value of stresses is observed at the junction of the weld zone and the thinner sheet. The stresses in the thinner sheet are always lower than in the thicker sheet for a given punch profile radius. The stress values at the mid layer before springback show increasing and decreasing trend on both tension and compression sides but majority of these stress values are below the yield strength of the material. The residual stress at the innermost integration points is compressive in nature, stresses in the thinner sheet are always lower than in the thicker sheet for all three given punch profile radius. Whereas, there is a sudden increase in the stress value is observed at the junction of thicker sheet and weld zone, although, the variation of stresses in weld zone is almost constant with slight decreasing-increasing variation and then there is a sudden decrease in the value of compressive stresses is observed at the junction of the weld zone and the thinner sheet.

As shown in figures 4.1(b), 4.2(b) and 4.3(b), it is observed that after springback, the residual stress at the outermost integration points on the thicker side is released and changes from tensile to compressive contrary to the case of before springback but the

stress on the thinner side is still tensile. This is due to the combined effect of thicker and thinner portions on the resultant springback of TWB. The thinner side was constrained from undergoing complete springback by the thicker side due to its higher stiffness and lower springback and hence the residual stress in the thinner is tensile. However, the value of stresses decreases for both thicker and thinner sheet. Weld zone shows the similar trend as before springback as there is sudden increase in the stress value at the junction of the thicker sheet and weld zone, then the stresses are constant throughout the weld zone with slightly decreasing-increasing variation and then there is sudden decrease in the stress value at the junction of the weld zone and thinner sheet. The residual stress at the innermost integration points on the thicker side become tensile contrary to the case of before springback but the stress on the thinner side is still compressive. However, the value of stresses for both the sides are lower than the before springback case. Whereas, there is a sudden decrease in the stress value is observed at the junction of thicker sheet and weld zone, although, the variation of stresses in weld zone is almost constant with slightly decreasing variation and then there is a sudden increase in the value of stresses that changes its nature from compressive to tensile, is observed at the junction of the weld zone and thinner sheet.

After springback, no significant change is observed in the stress distribution in the mid layer across the width of the specimen for all punch profile radii.

It is observed that as the punch profile radius increased, the longitudinal stress levels decreased on both tension and compression sides as shown in Fig. 4.1, 4.2 and 4.3. Higher stresses are seen on thicker side than on thinner side before springback in a given thickness combination for all the punch profile radii, whereas higher residual stress (compressive stress) after springback are observed on thicker side than on the thinner side (tensile stress).

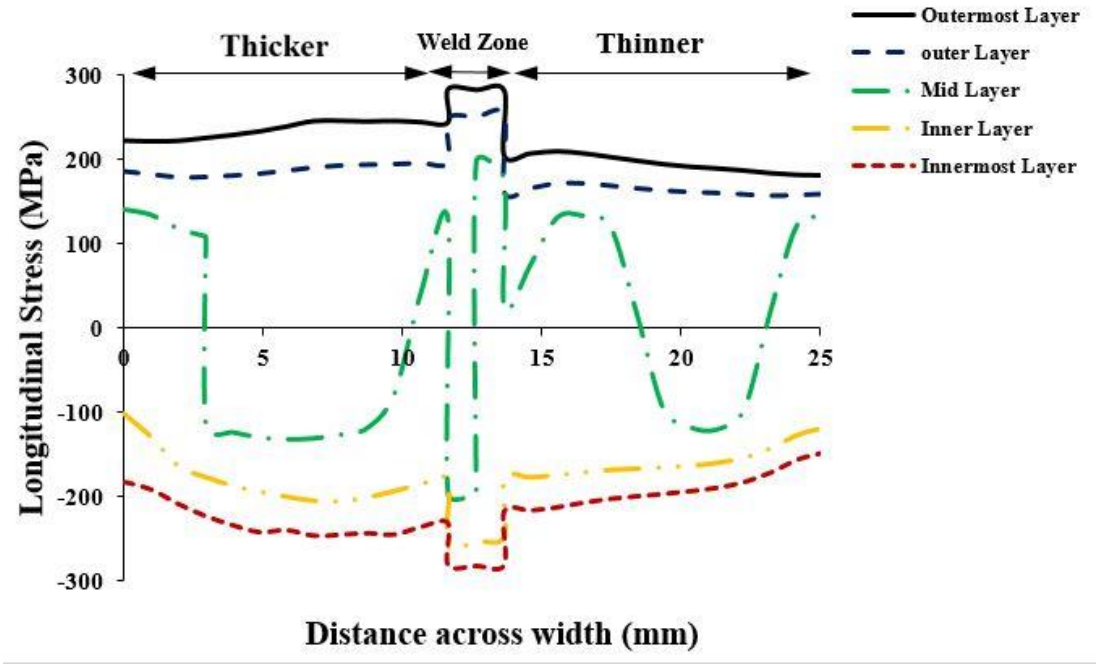

(a)

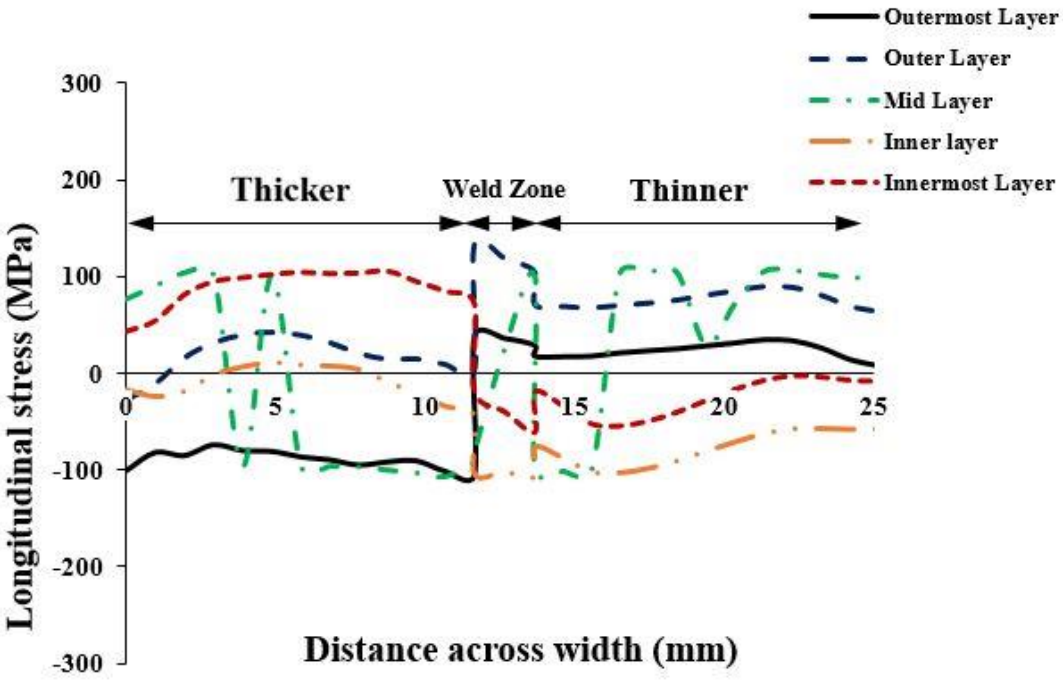

(b)

Fig. 4.1: Variation of longitudinal stress at different points through the thickness (a) before and (b) after springback across width of a TWB (0.8mmX1.5mm) for a punch profile radius of 10mm.

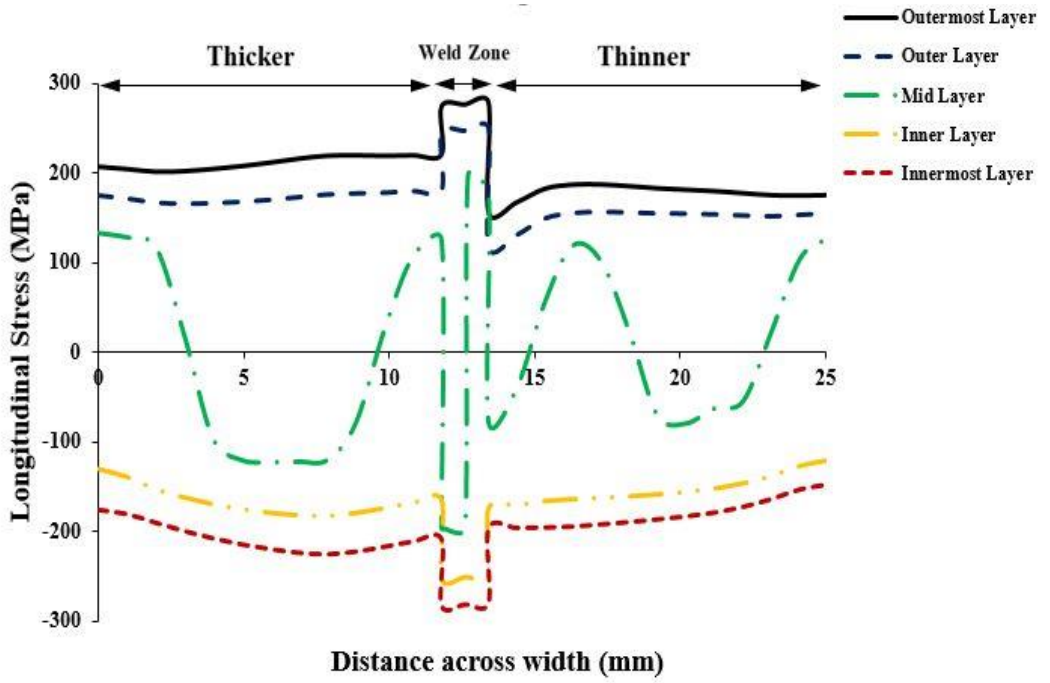

(a)

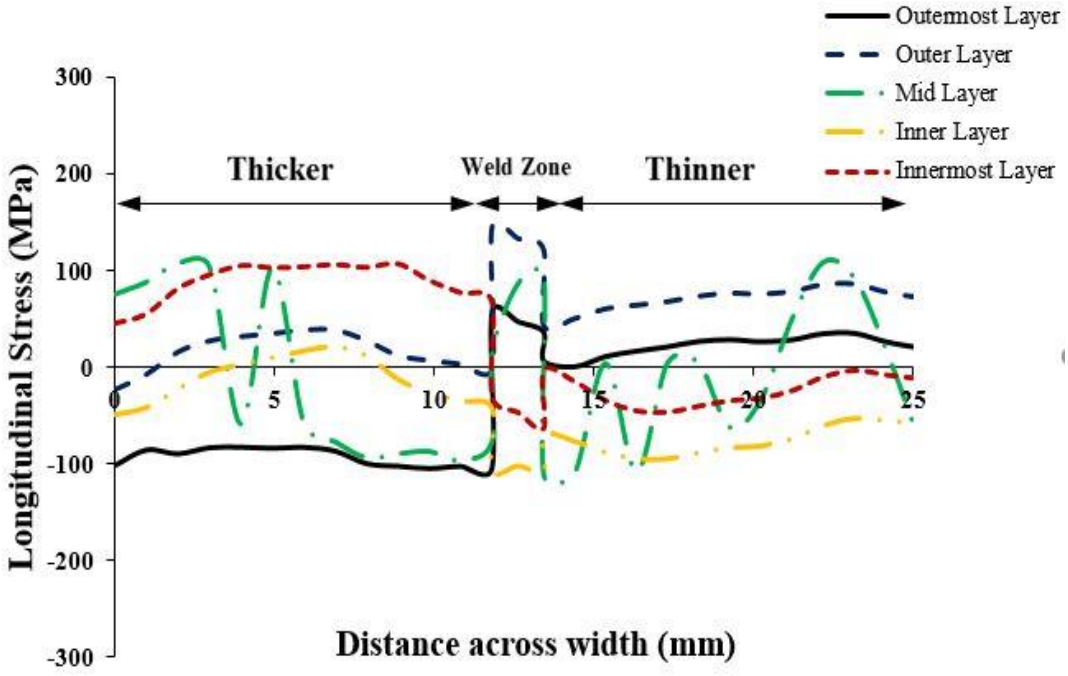

(b)

Fig. 4.2: Variation of longitudinal stress at different points through the thickness (a) before and (b) after springback across width of a TWB (0.8mmX1.5mm) for a punch profile radius of 12.5mm

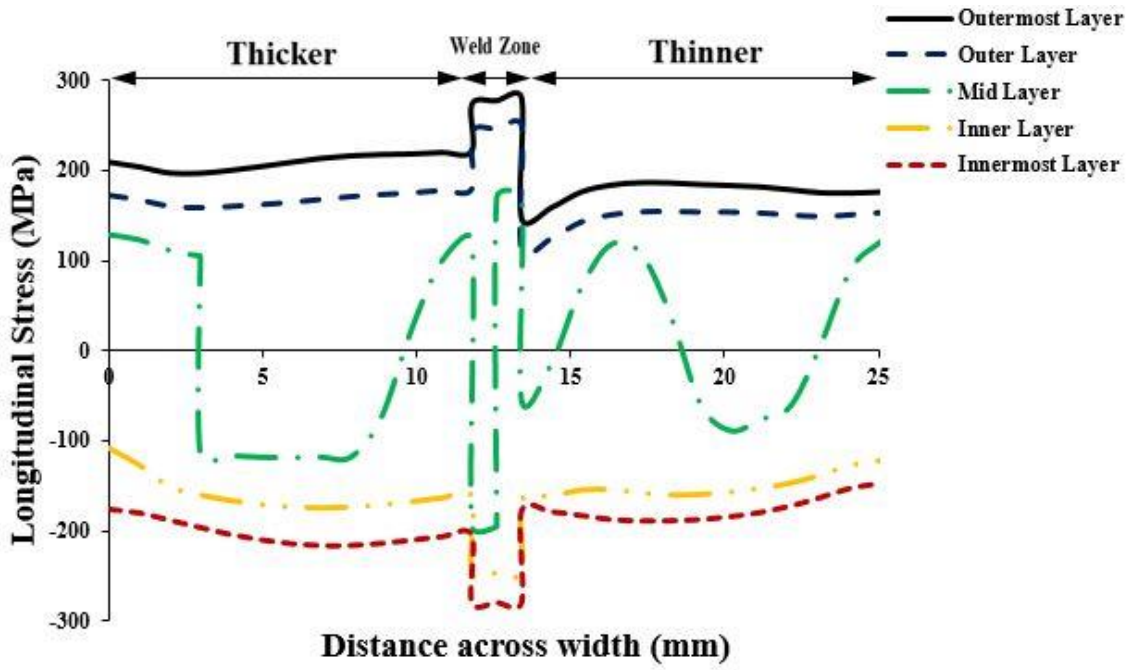

(a)

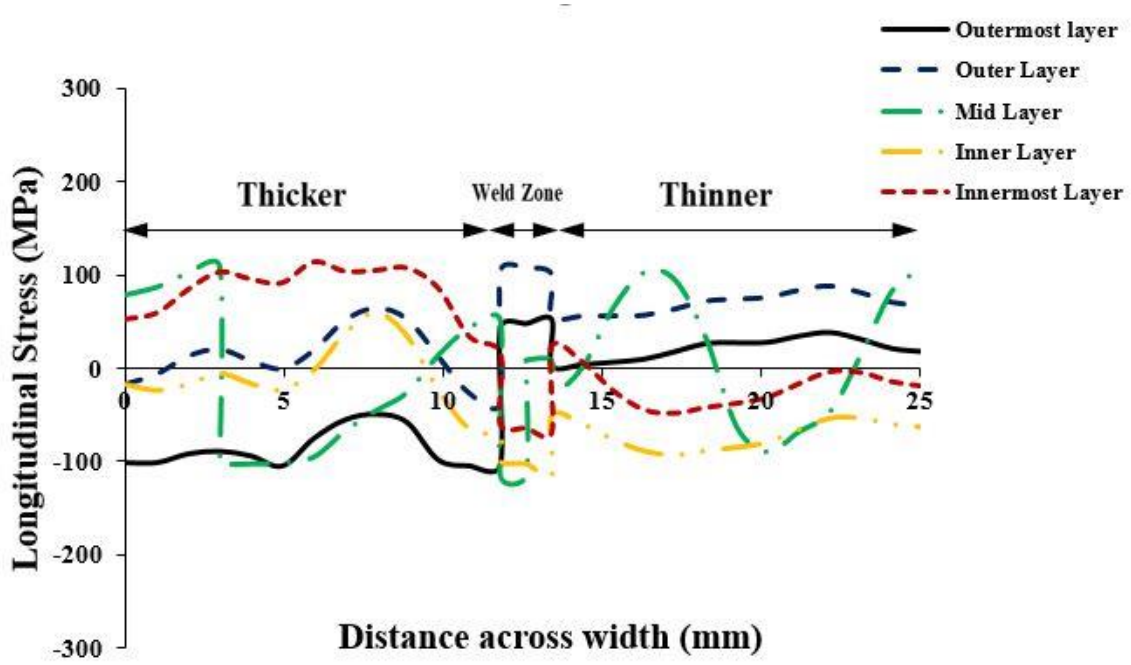

(b)

Fig. 5.3: Variation of longitudinal stress at different points through the thickness (a) before and (b) after springback across width of a TWB (0.8mmX1.5mm) for a punch profile radius of 15mm.

During the FEA simulation of the IF steel TWB (0.8mmX1.5mm) for three different punch profile radii 10mm, 12mm and 15mm the pattern of stress after bending and that of residual stress after springback is shown in figure 4.4, 4.5 and 4.6.

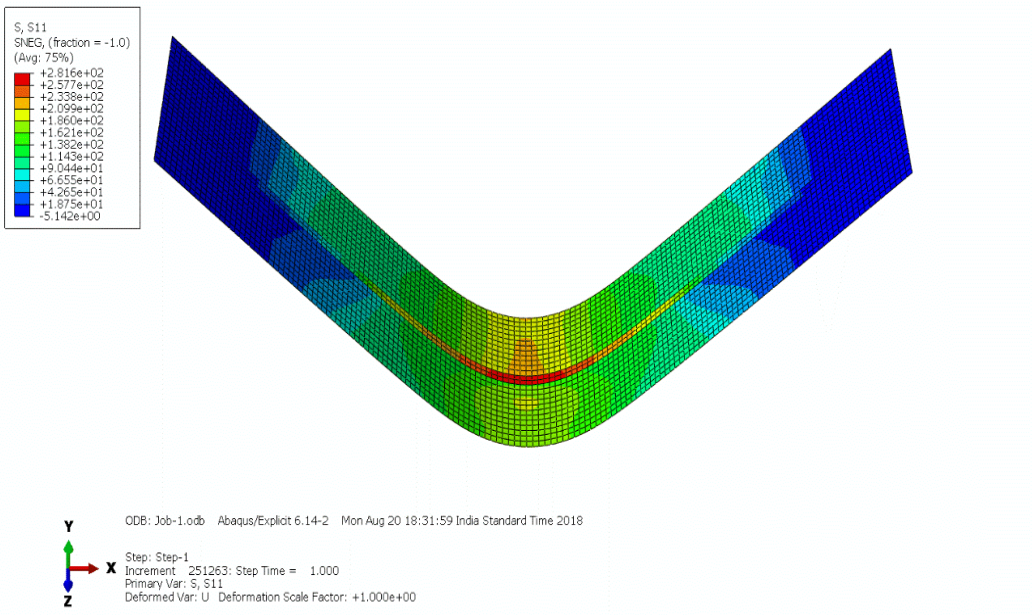

(a)

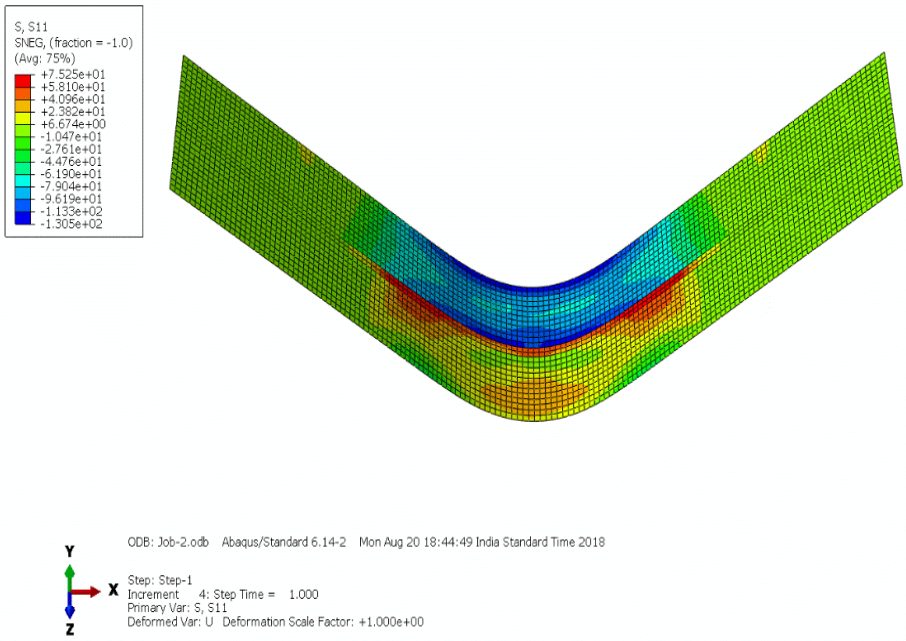

(b)

Fig. 4.4: FEA diagrams of TWB of IF steel for thickness combination of 0.8mm and 1.5mm (a) before springback and (b) after springback for the punch profile radius of 10 mm.

Fig.4.4 (a) shows the distribution of stresses after V-bending in the TWB for a punch of profile radius 10mm. It shows that the tensile stress induced at the weld region (red portion) with a maximum value of around +281 MPa. However, after springback or removal of punch force, stresses at weld region is relived but not completely and these still remaining stresses within the blank is known as residual stresses with a maximum value of around +75.25 MPa at the weld zone and its distribution is shown in fig.4.4 (b). The green region in the fig.4.4 (b) shows that the nature of stress is changed from tensile to compressive before and after springback respectively.

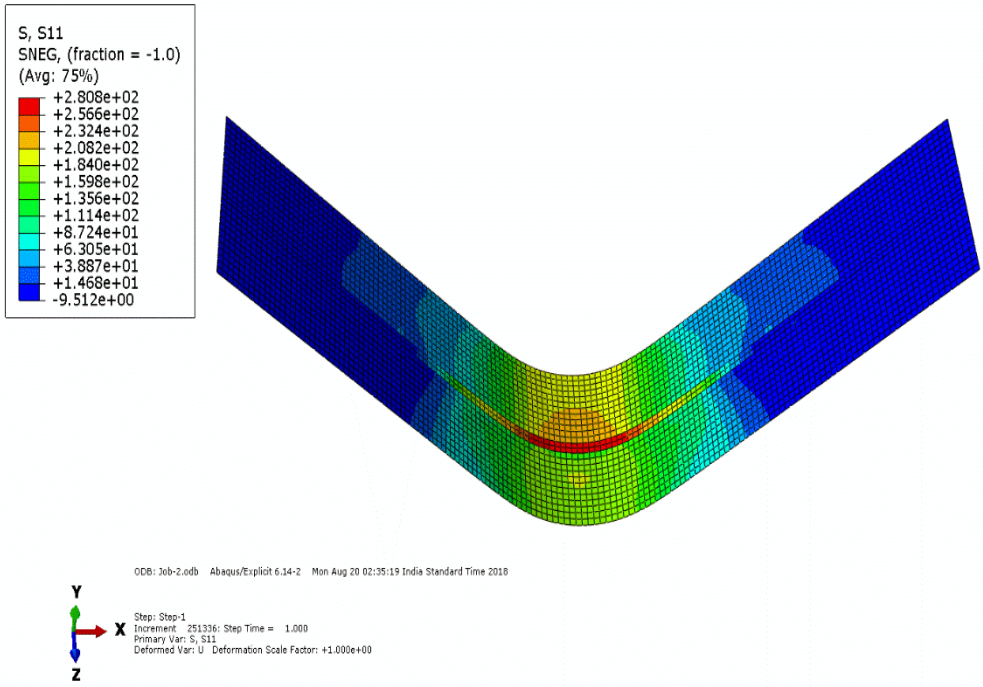

(a)

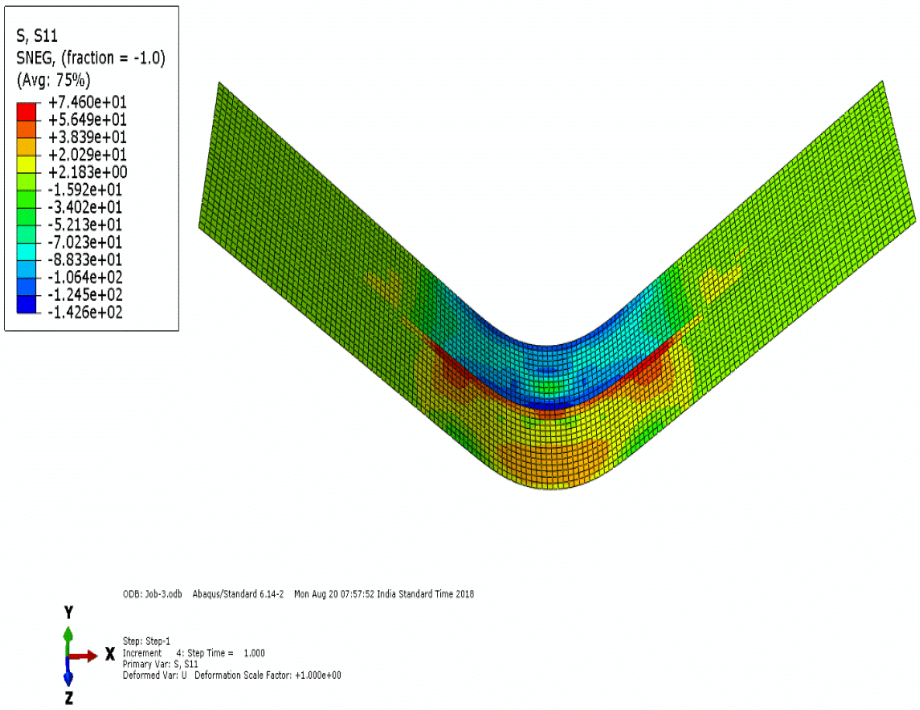

(b)

Fig. 4.5: FEA diagrams of TWB of IF steel for thickness combination of 0.8mm and 1.5mm (a) before springback and (b) after springback for the punch profile radius of 12.5 mm.

Fig.4.5 (a) shows the distribution of stresses after V-bending in the TWB for a punch of profile radius 12.5mm. It shows that the tensile stress induced at the weld region (red portion) with a maximum value of around +280 MPa. However, after springback or removal of punch force, stresses at weld region is relived but not completely and these still remaining stresses within the blank is known as residual stresses with a maximum value of around +74.6 MPa at the weld zone and its distribution is shown in fig.4.5 (b). The green region in the fig.4.5 (b) shows that the nature of stress is changed from tensile to compressive before and after springback respectively.

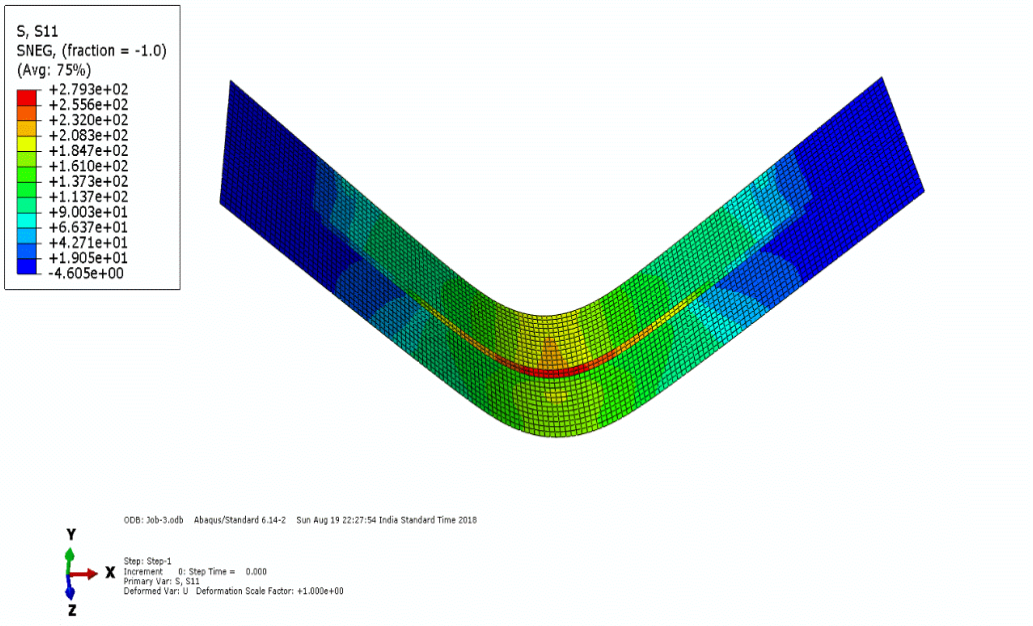

(a)

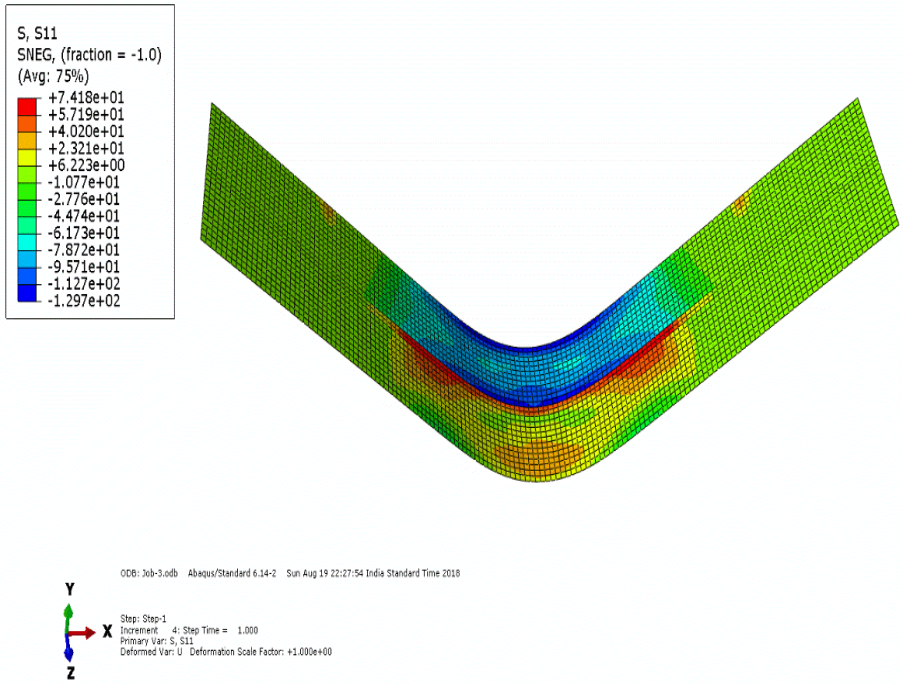

(b)

Fig. 4.6: FEA diagrams of TWB of IF steel for thickness combination of 0.8mm and 1.5mm (a) before springback and (b) after springback for the punch profile radius of 15 mm.

Fig.4.6 (a) shows the distribution of stresses after V-bending in the TWB for a punch of profile radius 15mm. It shows that the tensile stress induced at the weld region (red portion) with a maximum value of around +279 MPa. However, after springback or removal of punch force, stresses at weld region is relived but not completely and these still remaining stresses within the blank is known as residual stresses with a maximum value of around +74.18 MPa at the weld zone and its distribution is shown in fig.4.6 (b). The green region in the fig.4.6 (b) shows that the nature of stress is changed from tensile to compressive before and after springback respectively.

4.4 Validation of the predicted results with the experimental results

A comparison of residual stress values in the outermost and innermost surface layers of IF steel TWB (0.8mm×1.5mm) obtained from FE simulations after springback and experimental technique using cosα method for three different punch profile radii 10mm, 12.5mm and 15mm is given in Table 4.3.

As discussed, the values of residual stress obtained from FE simulations, on an average basis across the width of the specimen are in good agreement with the experimental values both in thinner and thicker sheet in a given thickness combination of 0.8mmX1.5mm for all punch profile radii. The residual stress in the thinner sheet is tensile in the outermost layer and compressive in the innermost layer but the thicker sheet is able to rearrange its stress distribution to compressive on outermost layer and tensile on innermost layer. As the profile radius increases, it is observed that residual stress value decreases in the outermost and innermost layer in the cases of both thicker and thinner sheets and the similar results are observed in experimental values. In experimental measurement of residual stresses, values at the weld zone of the TWBs is not determined as the width of weld zone is less than the spot diameter (2mm) of the incident X-ray.

Table 4.3: Comparison of experimental and predicted results

Punch Profile Radius (mm)	Location	Residual Stress (MPa)			
		Thinner		Thicker	
		FEA	EXP.	FEA	EXP.
10	Outermost Layer	49.98	56	-99.44	-75
	Innermost Layer	-38.1	-46	98.49	83
12.5	Outermost Layer	40.23	36	-94.62	-70
	Innermost Layer	-36.4	-21	93.53	31
15	Outermost Layer	25	16	-87.3	-46
	Innermost Layer	-33.6	-12	25.7	20

CHAPTER 5

CONCLUSIONS

In the present work, longitudinal stresses in TWBs (0.8mm×1.5mm) of IF steels before springback and residual stresses after springback are investigated for three different punch profile radius of 10mm, 12.5mm and 15mm. On the basis of the observations, the following conclusions are drawn:

1. Higher values of longitudinal stress before springback obtained from FE simulations is observed in the both outermost (tension side) and innermost layers (compression side) in the thicker sheet than the thinner sheet and a sudden drop in the values of stress is seen at the junction of the thicker sheet and weld zone and the weld zone and thinner sheet .
2. Longitudinal stress values before springback obtained from FE simulations decreases significantly as the punch profile radius increases. The reason for higher stress with smaller punch profile radius may be attributed to the smaller region of deformation and lower elastic core than with larger punch profile radius.
3. The effect of the punch profile radius on residual stress after springback is observed to be very significant in TWBs. As the punch profile radius increases, residual stress TWBs of IF steel with dissimilar thickness combination of 0.8mmX1.5mm decreases for a given thickness combination.
4. Residual stress predicted by FE simulations agreed well with the experimental results (without including the weld zone) for all punch radii.

CHAPTER 6

FUTURE SCOPE

In this work an FE model of TWB of IF steel is analyzed numerically for the different thickness combination along with the experimental result for the prediction of residual stresses. The future continuation of this work could analyze the effect of tensile and compressive residual stresses on the fatigue life by incorporating the experimental characterization of the various automotive components manufactured by the TWBs of IF steel. Also, the thorough mapping of the residual stresses before and after the springback at a certain distance from the weld zone of TWBs of IF steel will be beneficial in determination of the critical regions having higher values of tensile residual stresses. More work can be done with other grades of steels and with various other thickness combinations as they provide higher fuel efficiency and reduction in overall cost by reducing the weight of the vehicle.

REFERENCES

1. Merklein, M., Johannes, M., Lechner, M., & Kuppert, A. (2014). A review on tailored blanks—Production, applications and evaluation. *Journal of Materials Processing Technology*, *214*(2), pp.151-164.
2. Kinsey, B. L. (2011). Tailor welded blanks for the automotive industry. In *Tailor welded blanks for advanced manufacturing*, pp.164-180.
3. Anand, D., Chen, D. L., Bhole, S. D., Andreychuk, P., & Boudreau, G. (2006). Fatigue behavior of tailor (laser)-welded blanks for automotive applications. *Materials Science and Engineering: A*, *420*(1-2), pp.199-207.
4. Xu, F., Sun, G., Li, G., & Li, Q. (2014). Experimental investigation on high strength steel (HSS) tailor-welded blanks (TWBs). *Journal of Materials Processing Technology*, *214*(4), pp.925-935.
5. Song, Y., & Hua, L. (2014). Influences of thickness ratio of base sheets on formability of tailor welded blanks. *Procedia Engineering*, *81*, pp.730-735.
6. Gautam, V., & Kumar, D. R. (2017). Experimental and numerical investigations on springback in V-bending of tailor-welded blanks of interstitial free steel. *Proceedings of the Institution of Mechanical Engineers, Part B: Journal of Engineering Manufacture*, pp.1-14.
7. Rojek, J., Hyrcza-Michalska, M., Bokota, A., & Piekarska, W. (2012). Determination of mechanical properties of the weld zone in tailor-welded blanks. *archives of civil and mechanical engineering*, *12*(2), pp.156-162.
8. Dias, J. S., Chuvas, T. C., & Fonseca, M. D. P. C. (2016). Evaluation of residual stresses and mechanical properties of if steel welded joints by laser and plasma processes. *Materials Research*, *19*(3), pp.721-727.
9. Thasanaraphan, P. (2012). A Study on the Welding Characteristics of Tailor Welded Blank Metal Sheets Using GTAW and Laser Welding.
10. Wor, L. C., & Rahman, M. M. (2013). *Stress behavior of tailor-welded blanks for dissimilar metals using finite element method* (Doctoral dissertation, Universiti Malaysia Pahang).
11. Rossini, N. S., Dassisti, M., Benyounis, K. Y., & Olabi, A. G. (2012). Methods of measuring residual stresses in components. *Materials & Design*, *35*, pp.572-588.

12. Pineault, J. A., Brauss, M. E., & Eckersley, J. S. (1996). Residual Stress Characterization of Welds Using X-Ray Diffraction Techniques. *School of Materials and Mineral Resources Engineering Universiti Sains Malaysia, Perak Branch Campus 31750 Tronoh, Perak, Malaysia*, 97.

13. International Atomic Energy Agency. 2012. Measurement of residual stress in materials using neutrons.

14. Pineault, J. A., Brauss, M. E., & Eckersley, J. S. (1996). Residual Stress Characterization of Welds Using X-Ray Diffraction Techniques. *School of Materials and Mineral Resources Engineering Universiti Sains Malaysia, Perak Branch Campus 31750 Tronoh, Perak, Malaysia*, 97.

15. Ling, J., & Lee, S. Y. (2015). Characterization of a portable x-ray device for residual stress measurements. *Adv X-ray Anal, 59*, pp.153-161.

16. Peterson, N., Kobayashi, Y., Traeger, B., & Sanders, P. Assessment and Validation of Cosα Method for Residual Stress Measurement.

17. Clapham, L., Abdullah, K., Jeswiet, J. J., Wild, P. M., & Rogge, R. (2004). Neutron diffraction residual stress mapping in same gauge and differential gauge tailor-welded blanks. *Journal of materials processing technology*, *148*(2), pp.177-185.

18. Sasaki, T., Hirose, Y., Sasaki, K., & Yasukawa, S. (1997). Influence of image processing conditions of Debye Scherrer ring images in x-ray stress measurement using an imaging plate. *Adv. X-ray Anal, 40*, pp.588-594.

19. Zad Poor, A. A. (2010). *Tailor-made blanks for the aircraft industry* (Doctoral dissertation, TU Delft, Delft University of Technology).

20. Kopeliovich, D. pMax Black™: Strengthened Tri-metal Bearing Materials for High Performance Bearings.

21. Radaj, D. Heat effects of welding temperature field, residual stress, distortion, 1992.

22. Opbroek, E. G. (2009). Advanced high strength steel (AHSS) application guidelines: version 4.1. *World Steel Association, Brussels, Belgium, pv*.

23. Batterman, B. W., & Cole, H. (1964). Dynamical diffraction of X- rays by perfect crystals. *Reviews of modern physics*, *36*(3), pp.681.

24. Anderoglu, O. (2005). *Residual stress measurement using X-ray diffraction* (Doctoral dissertation, Texas A&M University).

25. Ling, J., & Lee, S. Y. (2015). Characterization of a portable x-ray device for residual stress measurements. *Adv X-ray Anal*, *59*, pp.153-161.

26. Fitzpatrick, M. E., Fry, A. T., Holdway, P., Kandil, F. A., Shackleton, J., & Suominen, L. (2005). Determination of residual stresses by X-ray diffraction.

27. Dölle, H. (1979). The influence of multiaxial stress states, stress gradients and elastic anisotropy on the evaluation of (Residual) stresses by X-rays. *Journal of applied Crystallography*, *12*(6), pp.489-501.

28. Ling, J., & Lee, S. Y. (2015). Characterization of a portable x-ray device for residual stress measurements. *Adv X-ray Anal*, *59*, pp.153-161.

29. Schajer, G. S. (2011). Destructive methods for measuring residual stresses: Techniques and opportunities. In *Experimental and Applied Mechanics, Volume 6*, pp. 221-231.

30. Withers, P. J., & Bhadeshia, H. K. D. H. (2001). Residual stress. Part 1–measurement techniques. *Materials science and Technology*, *17*(4), pp.355-365.

31. Withers, P. J., & Bhadeshia, H. K. D. H. (2001). Residual stress. Part 2–Nature and origins. *Materials science and technology*, *17*(4), pp.366-375.